MICROCOPY RESOLUTION TEST CHART

NATIONAL BUREAU OF STANDARDS-1963-A

AD-A156 296

AFWAL-TR-85-2016

ANALYSIS OF NON-EQUILIBRIUM EXCITATION IN PULSED
ELECTRIC DISCHARGES

L. C. Pitchford

GTE LABORATORIES, INC.
40 SYLVAN ROAD
WALTHAM, MASSACHUSETTS 02254

APRIL 1985

FINAL REPORT FOR PERIOD JUNE 1982 - SEPTEMBER 1984

DTIC
ELECTE
JUL 8 1985
B

AERO PROPULSION LABORATORY
AIR FORCE WRIGHT AERONAUTICAL LABORATORIES
AIR FORCE SYSTEMS COMMAND
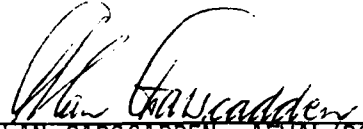WRIGHT-PATTERSON AIR FORCE BASE, OHIO 45433

85 6 2 017

NOTICE

When Government drawings, specifications, or other data are used for any purpose other than in connection with a definitely related Government procurement operation, the United States Government thereby incurs no responsibility nor any obligation whatsoever; and the fact that the government may have formulated, furnished, or in any way supplied the said drawings, specifications, or other data, is not to be regarded by implication or otherwise as in any manner licensing the holder or any other person or corporation, or conveying any rights or permission to manufacture use, or sell any patented invention that may in any way be related thereto.
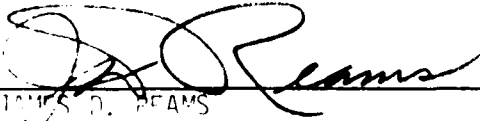
This report has been reviewed by the Office of Public Affairs (ASD/PA) and is releasable to the National Technical Information Service (NTIS). At NTIS, it will be available to the general public, including foreign nations.

This technical report has been reviewed and is approved for publication.

ALAN GARSCADDEN, AFWAL/POOC-3   PAUL R. BERTHEAUD, AFWAL/POOC
Plasma Physics Group   Chief, Power Components Branch
Power Components Branch   Aerospace Power Division
Aerospace Power Division   Aero Propulsion Laboratory
Aero Propulsion Laboratory

FOR THE COMMANDER

JAMES D. REAMS
Chief, Aerospace Power Division
Aero Propulsion Laboratory

"If your address has changed, if you wish to be removed from our mailing list, or if the addressee is no longer employed by your organization please notify AFWAL/POOC-3 W-PAFB, OH 45433 to help us maintain a current mailing list".

Copies of this report should not be returned unless return is required by security considerations, contractual obligations, or notice on a specific document.

REPORT DOCUMENTATION PAGE

1a. REPORT SECURITY CLASSIFICATION UNCLASSIFIED		1b RESTRICTIVE MARKINGS			
2a. SECURITY CLASSIFICATION AUTHORITY		3 DISTRIBUTION/AVAILABILITY OF REPORT Approved for public release; distribution unlimited.			
2b. DECLASSIFICATION/DOWNGRADING SCHEDULE					
4. PERFORMING ORGANIZATION REPORT NUMBER(S)		5 MONITORING ORGANIZATION REPORT NUMBER(S) AFWAL-TR-85-2016			
6a. NAME OF PERFORMING ORGANIZATION Sandia National Lab (GTE Research Lab)	6b OFFICE SYMBOL (If applicable)	7a NAME OF MONITORING ORGANIZATION Aero Propulsion Laboratory (AFWAL/POOC)			
6c. ADDRESS (City, State and ZIP Code) Sandia National Lab P. O. Box 5800 Albuquerque NM 87185		7b ADDRESS (City, State and ZIP Code) Aero Propulsion Laboratory (AFWAL/POOC) Air Force Wright Aeronautical Laboratories (AFSC)			
8a. NAME OF FUNDING/SPONSORING ORGANIZATION	8b. OFFICE SYMBOL (If applicable)	9 PROCUREMENT INSTRUMENT IDENTIFICATION NUMBER MIPR FY1455-82N0616			
8c. ADDRESS (City, State and ZIP Code)		10. SOURCE OF FUNDING NOS.			

	PROGRAM ELEMENT NO.	PROJECT NO.	TASK NO.	WORK UNIT NO.
	61102F	2301	S2	85

11. TITLE (Include Security Classification)

Analysis of Non-Equilibrium Excitation in Pulsed Electric Discharges (UNCL)

12. PERSONAL AUTHOR(S)

L. C. Pitchford

13a. TYPE OF REPORT Final Report	13b. TIME COVERED FROM 82/6 TO 84/9	14. DATE OF REPORT (Yr., Mo., Day) 85/04/25	15. PAGE COUNT 77

16. SUPPLEMENTARY NOTATION

17.	COSATI CODES		18. SUBJECT TERMS (Continue on reverse if necessary and identify by block number)
FIELD	GROUP	SUB. GR.	Electron; distribution function; time-dependent Boltzmann equation; ionization rate; model cross-section,
20	3	22	
20	9	4	

19. ABSTRACT (Continue on reverse if necessary and identify by block number)

A numerical solution of the time-dependent Boltzmann equation has been tested with model calculations. Some comparisons were made with nitrogen cross-sections. The model calculations are relatively fast and much easier to analyze. The electrons lose memory of their initial conditions for times greater than the energy exchange time. This relaxation time can vary orders of magnitude depending on the gas composition and the ratio of the applied field to the total gas density (E/N). The limits on the applicability of the local field approximation have been explored. It is found that it is a valid parameter for coefficients in the electron continuity equation provided E/N does not change within a few energy exchange times. Several attempts have been made to find a parameterization of the time-dependent transport and rate coefficients, or to formulate a hydrodynamic-like model for time-dependent fields. Previous efforts to describe, for example, the ionization rate in the nonuniform field region of a discharge, have been examined for application in the time-dependent problem. However, the study did not find such a description for the

20. DISTRIBUTION/AVAILABILITY OF ABSTRACT UNCLASSIFIED/UNLIMITED ☒ SAME AS RPT. ☐ DTIC USERS ☐	21. ABSTRACT SECURITY CLASSIFICATION UNCLASSIFIED	
22a. NAME OF RESPONSIBLE INDIVIDUAL Dr Alan Garscadden	22b TELEPHONE NUMBER (Include Area Code) (513) 255-2923	22c. OFFICE SYMBOL AFWAL/POOC-3

DD FORM 1473, 83 APR EDITION OF 1 JAN 73 IS OBSOLETE.

time-dependent case.

The electron continuity equation only requires information on the electron density growth (or decay) constants and the electron flux. By restricting the information sought from the electron energy distribution function to the growth constants and the flux, phenomena which may be important in some applications are not observed. For example, while the net electron current is sensibly directed towards the anode throughout the relaxation of the electron energy distribution function, there is a component of the current which flows to the cathode and which consists of the low velocity electrons. The moments which are most sensitive to this component are not usually included in models of gas discharges.

FOREWORD

Accession For

NTIS GRA&I

DTIC TAB

Unannounced

Justification

By

Distribution/

Availability Codes

Avail and/or

Dist   Special

A-1

TABLE OF CONTENTS

LIST OF ILLUSTRATIONS

LIST OF ILLUSTRATIONS (Concluded)

I. Introduction

Transport and rate coefficients defining the properties of an electron swarm interacting with a weakly ionized gas and under the influence of an electric field are well parameterized by E/N, the ratio of the electric field strength to the neutral gas density, for uniform fields in time and space and when the electron swarm has lost memory of its initial conditions. Under this contract we have developed a numerical solution of the time-dependent Boltzmann equation for electrons in a weakly ionized gas to study the departures from the simple E/N parameterization for time-dependent fields or in the presence of sources of electrons. The spatially homogeneous, time-dependent Boltzmann equation was solved to give the electron energy distribution function (EEDF) for a variety of model gases and for nitrogen. A description of the time-dependent Boltzmann equation and the solution technique is given in Section II.

An appropriate choice of model gases with simple electron-neutral interactions allows us to examine qualitatively all the transient phenomena that occur in more realistic gas models while retaining computational simplicity. With the use of simple models, some analytical results are possible and are useful as a guide to the understanding of the underlying physics in the transient regime. With the more realistic gas models, the physics is often buried in the details. Comparisons of the numerical results with the analytical solutions also provide rigorous tests of the numerical methods used in the computer solution of the Boltzmann equation. These comparisons are discussed in Section III.

Several interesting transient phenomena which proved to be quite general were found in the model studies. For example, we saw overshoots and under-shoots in the transient electron drift velocities which have analogues in hot carrier transport in semiconductors (Reference 1). Associated with these transient phenomena is a cathode-directed component of the current which results from cooling in certain regions of the electron energy distribution. In

general, the macroscopic averages over the energy distribution function such as the rate coefficients are not monotonically increasing or decreasing functions of time. There can be oscillations present, although these are usually rather small. A discussion of these phenomena is also given in Section III.

A timely application of these types of calculations is found in the problem of microwave propogation through the atmosphere. Here, the concern is very-fast rising and high-power microwave breakdown in the atmosphere. Microwave excitation of gas discharges is usually described by an effective field which allows scaling from DC results (Reference 2). We have performed the time-dependent Boltzmann calculations using the full time-dependence of the microwave fields. Results of these calculations are presented and compared with the conventional models in Section IV. This work has been the basis for the design and analysis of an experiment at Sandia National Laboratories to measure the temporal growth of current after application of a fast rising microwave pulse (Reference 3). The very good comparison with experiment gives us confidence in the numerical methods and input cross section data.

Extensive compilations of measured and calculated electron swarm data exist as functions of E/N for a variety of gases and gas mixtures (References 4, 5). The utility of these data is in the simple parameterization and hence applicability of the data to a wide variety of experimental situations. Through calculations here, we have attempted to quantify the limits of validity of the E/N parameterization for time-dependent fields. If the field varies rapidly, the transport and rate coefficients are no longer functions of only E/N and the gas composition, but also of time. It is desirable to find a way to either modify the extensive swarm data base to include in some macroscopic way the time dependence of these swarm parameters or to find a parameterization better suited for a macroscopic description of the time-dependent phenomena. In Section V we present several attempts to formulate a hydrodynamic model to use instead of the full kinetic (Boltzmann or Monte Carlo) description when the fields are varying in time.

Questions analagous to those raised for time dependent excitation of discharges can also be asked in the case of spatially dependent fields. Monte Carlo calculations have been initiated to study electron transport in spatially varying fields. We find effects (overshoots, undershoots, cathode-directed current components, non-monotonic relaxation, etc.) quite analagous to those seen in the time dependent calculations (Reference 6). A summary of this work, conclusions and implications to other problems are presented in Section VI.

Of the many previous calculations of time-dependent EEDF's, we present here only a brief outline of the major points. Previous time-dependent calculations can be divided into three main categories; electron thermalization (field-free), approach to steady-state (finite field), and high frequency excitation. A good review of this work through 1979 is given by Wilhelm and Winkler (Reference 7).

There has been quite a bit of both numerical and analytical work related to the problem of electron thermalization in gases (References 8-13). The context of much of the previous work on electron thermalization has been the relaxation of a beam of electrons injected into a gas. The analytical results presented in Section III are consistent with the previous analytical results where comparisons are possible, but our results are more general than the previous work for certain classes of problems.

Wilhelm and Winkler and their coworkers have published a number of papers (Reference 14) related to the approach to steady-state; i.e, the relaxation of the EEDF, in which they have solved the two-term form of the time-dependent Boltzmann equation for a variety of atomic and molecular gases. Their results are consistent with those in Section IV in that the steady-state is achieved in times related to the energy relaxation frequencies and more or less independently of the initial conditions. These times can vary orders of magnitude depending on the gas and the values of the field. Braglia and his coworkers (References 11, 15) and Tagashira and his coworkers (References 16, 17) nave

3

also looked at the approach to steady-state using both Boltzmann and Monte Carlo techniques. Where the Boltzmann equation has been used in these investigations, it has always been in the form of a time-dependent, second-order differential equation for the isotropic part of the distribution.

Wilhelm and Winkler (Reference 18) have published the only detailed calculations, to our knowledge, of time-dependent EEDF's as a result of microwave excitation of an electron swarm. They maintain the full time-dependence of the field rather than resorting to the effective field model, but they use the standard two-term form of the Boltzmann equation for these calculations as well as for their DC field calculations.

There are many other time-dependent Boltzmann calculations and several computer codes are available to do the problem (Reference 19). In fact, any iterative solution of the Boltzmann equation is in some sense a time-dependent solution. These codes have been used to calculate EEDF's when electron-electron collisions are important, for example. They have not been used in any systematic way to investigate the transient phenomena or electron transport in time-dependent fields.

Unique features of the work here are: (1) a more general form of the time-dependent Boltzmann equation than in the previous calculations is used here, (2) the analytical results in Section III provide an insight to the time-dependent phenomena, and most importantly, (3) these calculations are intended to form the basis of a study of electron transport in time-dependent fields as well as of the approach to steady-state.

II. Formulation of the Boltzmann Equation and Solution Technique

The Boltzmann equation for electrons under the influence of an electric field and interacting with a weakly ionized gas can be written (Reference 20);

$$\frac{\partial f}{\partial Nt} + \frac{\vec{v}}{N} \cdot \nabla_r f + \frac{\vec{a}}{N} \cdot \nabla_v f = C[f] \qquad (1)$$

where $f(\vec{r},\vec{v},t)$ is the electron energy distribution function (EEDF) which depends on the spatial coordinates, $\vec{r}$, the velocity vector, $\vec{v}$, and time, t. The acceleration due to the field is $a = -e|E|/m$, and C is the collision operator discussed below. This equation provides a full statistical description of the microscopic behavior of an electron swarm interacting with a gas and subjected to an electric field which may be a function of time or space. Factors of N, the neutral density, are explicitly included throughout this report to illustrate the scaling; i.e, the space and time parameters always enter in products with the density.

When the electrons have lost memory of their initial conditions and if the fields are uniform in space and time, the hydrodynamic approximation is assumed to provide an accurate description of the space-time evolution of the electron swarm. The hydrodynamic approximation can be expressed (Reference 21),

$$f(\vec{r},\vec{v},t) = \sum_j f^{(j)}(\vec{v}) \otimes (-\nabla)^j n_e(\vec{r},t) \qquad (2)$$

where n_e, the electron density, is,

$$n_e(\vec{r},t) = \int f(\vec{r},\vec{v},t) \, d\vec{v}$$

The term "hydrodynamic", when refering to electron transport in weakly ionized gases, implies a constant exponential growth or decay of the electron density and that the space-time dependence of the EEDF is fully carried in $n_e(\vec{r},t)$ (Reference 21). This is expressed by eq.(2). In practice and in constant fields, this means that the transport and rate coefficients are functions only of E/N and the gas composition.

An equivalent expression of the hydrodynamic condition for a steady-state situation is (Reference 16, 22),

$$f(\vec{r},\vec{v}) = e^{\alpha z} f_{ss}(\vec{v})$$

(3)

where α is the spatial growth (or decay) constant.

The one-dimensional electron continuity equation in the hydrodynamic regime can be written as,

$$\frac{\partial n_e}{\partial Nt} = \frac{\nu_i}{N}\left(\frac{E}{N}\right) n_e - v_d\left(\frac{E}{N}\right)\frac{\partial n_e}{\partial Nz} + D_L N\left(\frac{E}{N}\right)\frac{\partial^2 n_e}{\partial (Nz)^2} + \ldots$$

(4)

where ν_i/N is the reaction rate coefficient, v_d is the drift velocity and D_L is the longitudinal diffusion coefficient. Equation (4) is the 0th velocity moment of eq.(1) and the coefficients in eq.(4) can be identified as various integrals over the EEDF.

6

A feature of the hydrodynamic regime is that the coefficients in the electron continuity equation are functions only of E/N and are independent of space and time. When the externally applied field is a slowly varying function of space or time, it is supposed that the EEDF responds immediately to changes in the field and that the coefficients in the continuity equation can be written as functions of the local, instantaneous value of E/N; e.g., $\nu_i(z,t) = \nu_i(z,t) = \nu_i(E(z,t)/N)$. The basis of this is the assumption that the EEDF is a function of the local field and thus all averages over the EEDF are functions of the local field.

If the fields are rapidly varying functions of time or space, the EEDF will also depend on time or space because it cannot instantaneously adjust to changing fields. In addition, if there are external sources of ionization, the EEDF will also depend on those sources. Our interest here is in the response of the EEDF to rapidly varying fields in time and it has been shown that the continuity equation for that case can be written as (Reference 17, 23),

$$\frac{\partial n_e}{\partial Nt} = \frac{\nu_i}{N}(t) \, n_e \; - \; v_d(t) \frac{\partial n_e}{\partial Nz} \; + \; D_L N(t) \frac{\partial^2 n_e}{\partial (Nz)^2} \; + \; \ldots \tag{5}$$

All averages over the distribution; e.g., the excitation rate coefficients, will depend on the same parameters as do the coefficients in the electron continuity equation. Except where there is electron runaway, the long time limit of eq.(5) after the field has been changed to a new value is given by the hydrodynamic continuity equation.

7

The calculations here are of time-dependent, spatially-independent EEDF's. These EEDF's can be thought of as 0th spatial moments or as coefficients in the time-dependent equivalent of eq.(2); i.e.,

$$f(\vec{r},\vec{v},t) = \sum_j f^{(j)}(\vec{v},t) \otimes (-\nabla)^j n_e(\vec{r},t).$$

Thus, the form of the Boltzmann equation that is solved here is,

$$\frac{\partial f^{(0)}(\vec{v},t)}{\partial Nt} + \frac{a}{N} \frac{\partial f^{(0)}(\vec{v},t)}{\partial v_z} = C[f^{(0)}(\vec{v},t)]. \tag{7}$$

The method used for the solution of the Boltzmann equation is an extension of a previously developed technique in which the angular dependence of the velocity is approximated by a Legendre expansion (Reference 24),

$$f^{(0)}(\vec{v},t) = \sum_i f_i(\vec{v},t) P_i(\cos\theta). \tag{8}$$

For isotropic electron-neutral scattering, the collision operator is given explicitly as,

$$C[f_0(v,t)] = -\sum_k Q^k(v) v f_0(v,t) + \frac{m}{M} \frac{1}{v^2} \frac{\partial}{\partial v}[Q^0(v)v^4 f_0(v,t)]$$

$$\tag{9a}$$

$$+\sum_k \frac{v_k^2}{v} Q^k(v_k) f_0(v_k,t) + \frac{4v_{ion}^2}{v} Q^{ion}(v_{ion}) f_0(v_{ion},t)$$

8

$$C[f_i(v,t)] = -Q^T(v) f_i(v,t) \quad , \quad i > 0. \tag{9b}$$

A full description of the derivation of this collision integral can be found in references 20, 24 and 26. The Q^k's are the cross sections for electron-molecule elastic ($k=0$), inelastic (k) and ionizing ($k=ion$) collisions. The total cross section, Q^T, is the sum of elastic, inelastic, ionizing and attaching collisions. The velocities v_k are related to the energy loss ε_k in the kth inelastic process,

$$v_k = (\varepsilon + \varepsilon_k)(2e/m)^{\frac{1}{2}}$$

and v_{ion} is related to the ionization potential ε_{ion} by,

$$v_{ion} = (2\varepsilon + \varepsilon_{ion})(2e/m)^{\frac{1}{2}}.$$

There is no scattering-in term due to attachment because electrons are lost to the distribution as a result of an attaching collision. Two electrons are scattered-in as a result of an ionizing collision, and we have assumed in writing the ionization contribution to the scattering-in that the two electrons exiting the ionization event share equally the excess energy of the primary over the ionization potential. This approximation has been discussed before and has been found to be quite good up to relatively high E/N in N_2 (Reference 21).

Although the solution method developed here is general, the results reported are for a two-term approximation. Several spot checks were made along the way to verify that the two-term approximation introduces no more error in the transient regime than it does in the time-independent cases (References 22, 24), and this was found to be the case.

A convenient way to include anisotropic electron-molecule scattering is through the Legendre components of the differential scattering cross sections (Reference 22),

$$Q_i^k = \frac{d\sigma_k(v,\theta)}{d\Omega} \; P_i(\cos\theta) \; d\Omega, \tag{10}$$

and,

$$C[f_i(v,t)] = -Q_0^T(v) \; v \; f_i(v,t) + \sum_k \frac{v_k^2}{v} \; Q_i^k(v_k) \; f_i(v_k,t) \tag{11}$$

$$+ \frac{4v_{ion}^2}{v} \; Q_i^{ion}(v_{ion}) \; f_i(v_{ion},t), \; i > 1.$$

The method described can include anisotropic scattering through use of the Q_i^k's, but we present only qualitative results with anisotropic scattering here. Calculations in the hydrodynamic regime up to moderately high E/N in N_2 (Reference 22) have not convinced us that it is necessary to go to the effort of including the anisotropic scattering except when precision results are required.

For the computer solution, equation (7) is written in vector form,

$$\frac{\partial F_i(v,t)}{\partial Nt} = \sum_{j,m} A_{ij} \; D_{jm} \; F_m(v,t) + \sum_{j,m} B_{ij} \; D_{jm} \frac{\partial F_m(v,t)}{\partial v}$$

$$+ \sum_{k,j} C_{ij}(v_k) \; F_j(v_k,t) + S(v,t) \tag{12}$$

10

where $F = (f_0, f_1, \ldots)$. The A, B and D matrices are time-independent and tridiagonal. C is a time-independent, diagonal matrix that accounts for the scattering-in terms in the collision integral. S is a vector to describe any external sources. Sources have not been included so far in the calculations. The non-zero elements of A, B, and C are;

$$A(1,1) = Q^0 v + mv/M \ (v \ dQ^0/dv + 4Q^0) \ ,$$

$$A(i,i) = -Q^T v \ , \quad i \neq 1 \ ,$$

$$A(i,i+1) = -a(i^2 + 3i + 2)/(v(2i+3)) \ ,$$

$$A(i,i-1) = a(i^2 - i)/(v(2i-1)) \ ,$$

$$B(1,1) = v^2 m Q^0/M \ ,$$

$$B(i,i) = 0, \quad i \neq 1 \ ,$$

$$B(i,i+1) = -a(i+1)/(2i+3) \ ,$$

$$B(i,i-1) = -a(i)/(2i-1) \ ,$$

$$C(i,i)(v_k) = Q^k_i(v_k)(v_k^2/v) \ ,$$

$$C(i,i)(v_{ion}) = 4Q^{ion}_i(v_{ion})(v_{ion}^2/v) \ .$$

Because these matrices are time-independent, their elements are evaluated only once during the calculation. The time dependence of the RHS is included in the D matrix. For a time dependent field where $E(t) = E_0 G(t)$, the non-zero elements of the D matrix are,

$$D(i,i\pm1) = G(t) \ ,$$

$$D(i,i) = 0 \ .$$

11

The solution was found by integrating each component of eq.(12) using a variable order Adams-Bashforth-Mouton predictor-corrector algorithm (Reference 27). An implicit integration algorithm was necessary for stability.

There were several numerical problems that came up in the implementation of the solution technique outlined above. For example, the F's are defined on a velocity grid and the velocity derivatives of the F's must be calculated at each time step in the integration. Further, there is no constraint of positivity on the distribution function in the integration scheme. A problem that is still outstanding is the implementation of a "breathing" grid in velocity space to allow the distribution function to grow several orders of magnitude in velocity space during the course of its evolution and still maintain accuracy in the early times.

The calculation of the derivatives was made more accurate by avoiding the point v=0 in the velocity grid where the odd Legendre components of the EEDF are singular (Reference 28). The velocity grid starts at some small but finite velocity. Derivatives calculated using splines are difficult because analytic behavior at the end points must be built into the spline basis set. We were not able to find any general analytic forms for the derivatives at the end points in the transient regime. The most stable results were found using finite differences with the constraint that the distribution function is continuous through $v_z = 0$ where v_z is the velocity in the field direction. This is physically justifiable and was found to be very solid numerically. Without this constraint, finite differences for the derivatives introduced so much error that the integration routine could not find a solution to within the prescribed accuracy at late times. The distribution function and its velocity derivatives at the high energy end were assumed to go to zero.

Positivity of the distribution function was forced by using the logorithm of f_0 in the calculation. The higner Legendre components can be positive or negative and therefore we use the components themselves in the calculations.

Several attempts were made to construct a time-dependent velocity grid. We have not yet succeeded in implementing this option, although there is no reason it cannot be done. Accumulation of numerical error has been a severe problem in the schemes tried so far.

The solution scheme presented here is more general than the several previous time-dependent Boltzmann calculations (References 14, 18, 19). We are not restricted to a two-term Legendre expansion of the velocity dependence of the distribution function and as much detail as is desired can be included in the differential cross section data describing the interaction of the electrons with the neutral gas particles. Most importantly, we do not assume that all the angle moments are in equilibrium with the isotropic component of the EEDF. Although these previous approximations are not bad, as will be seen, the usual form of the Boltzmann equation that has been used previously; i.e., one second order differential equation for f_0, is not the most convenient form for examining the underlying physics and the transient phenomena.

III. Model Results

In this section results of numerical and analytical calculations are presented for the time-dependent EEDF and rate and transport coefficients in several simple model gases. Where, to the author's knowledge, the analytical results have not been previously published, more detail is given.

1. Zero Field, Power Law Cross Sections

In the absence of an electric field, a swarm of hot electrons will eventually cool to a maxwellian at the gas temperature. We study here a simplified model of this situation in which the gas temperature is zero and the only electron-neutral scattering processes are elastic (Reference 29). Further, the cross section is assumed to be isotropic and to depend on some integer power n of the electron velocity. This model is mostly of theoretical interest, but it provides a stringent test of the numerical method and some qualitative insight to the relaxation.

After expansion of the EEDF in a Legendre series, the Boltzmann equation for the field-free cooling problem may be written as a set of uncoupled differential equations (any coupling of the angular parts of the velocity is due to the field),

$$\frac{\partial f_0}{\partial Nt} = \frac{1}{v^2} \frac{m}{M} \frac{\partial}{\partial v} [Q_0^0 v^4 f_0] , \tag{13}$$

$$\frac{\partial f_i}{\partial Nt} = -Q_0^0 v f_i , \quad i > 0. \tag{14}$$

The solution of eq. (14) is,

$$f_i (v,t) = f_i (v,o) \exp (-Q_0^0 v Nt). \tag{15}$$

14

A general solution of eq. (13) by be found by first defining a function g

$$g = \frac{m}{M} \, Q_0^0 \, v^4 \, f_0$$

and a new velocity variable $\tau = \tau(v)$ such that,

$$\frac{\partial g}{\partial N t} = \frac{\partial g}{\partial N \tau} .$$

The general solution for g is,

$$g(v,t) = F(t + \tau)$$

where

$$F(o + \tau) = \frac{m}{M} \, Q_0^0 \, v^4 \, f_0 (v,o).$$

For an electron scattering cross section of the form,

$$\frac{m}{M} \, Q_0^0 = q v^n$$

the variable τ can be expressed in terms of the velocity,

$$\tau(v) = \int_0^v \frac{dv'}{q v'^{n+2}} = \frac{-(n+1)}{q v^{n+1}} \quad , \quad n > -1.$$

Conversely, the expression for v in terms of τ is,

15

$$v(\tau) \;=\; \left[\frac{-(n+1)}{q\tau} \right]^{1/(n+1)} .$$

Then,

$$F(0,\tau) \;=\; q\, v^{n+4}\, f_0\,(v,0)$$

$$=\; q\, \left(\frac{-(n+1)}{q\tau} \right)^{(n+4)/(n+1)} f_0 \left[\left(\frac{-(n+1)}{q\tau} \right)^{1/(n+1)} , 0 \right],$$

from which it follows that

$$F(t+\tau) = q\, v^{n+4}\, \left(\frac{(n+1)}{r+1 - qtv^{n+1}} \right)^{(n+4)/(n+1)} f_0 \left[\left(\frac{n+1}{n+1 - qtv^{n+1}} \right)^{1/(n+1)} , 0 \right].$$

Let

$$y \;=\; \left(\frac{n+1}{n+1 - qtv^{n+1}} \right)^{1/(n+1)} ,$$

then

$$F(t+\tau) = q\, (yv)^{n+4}\, f_0\,(yv,0).$$

16

Imposing the condition of normalization, we find the general solution for $f_0(v,t)$,

$$f_0(v,t) = \begin{cases} y^4 f_0(yv,0) & y > 0 \\ 0 & y \leq 0 \end{cases} \qquad (16)$$

where

$$y = \begin{cases} \left(\dfrac{n+1}{n+1 - qtv^{n+1}} \right)^{1/(n+1)} & n > -1 \\ \exp(Q_0^0 \, vNt) & n = -1 \\ 0 \; . & n < -1 \end{cases}$$

There are no normalizable solutions for $n < -1$ because the collision frequency goes to zero at high energies. Thus the constant collision frequency, $n=-1$, represents a limit of how fast the cross section can decrease with velocity and still lead to a physical solution for the EEDF even for a zero field. We will see further examples of the unique behavior for $n=-1$ in finite fields. The cut-off at $y=0$ in eq.(16) follows by noting that the normalization in velocity space must be independent of time since in this model no electrons are created or destroyed.

There are several interesting points to be noted in the above solutions. The first point is that an initial delta function distribution function preserves its shape throughout the relaxation. This was discussed by Eaton and Holoway (Reference 10) and Braglia (Reference 11). and is particular to the assumption of a zero gas temperature. During the relaxation of an initial delta function EEDF the monoenergetic velocity at any time t for a constant cross section model, $n=0$, can be written,

$$v(t) = v(t=0) \left[1 + v(t=0) \, qNt \right]^{-1}$$

and the corresponding electron energy as a function of time is,

$$\epsilon(t) \; = \left(\frac{m}{2e}\right)\left(\frac{v(t=0)}{1+v(t=0)\;qNt}\right)^2$$

The average velocity and energy thus relax, not exponentially, but with powers of time. The average energy also depends on powers of time for other initial distributions as well, and in particular for a Druyvestynian. Such a power law dependence of the relaxation indicates a continuous spectrum of eigenvalues.

Note also that if the initial EEDF is maxwellian,

$$f_0(v,0) = A \; \exp(-Bv^2)$$

then, for n=-1,

$$f_0\,(v,t) \; = \; [\exp(vt)]^3 \; f_0\,[v \; \exp\,(vt),\; o]\;.$$

i.e., an initial maxwellian also preserves its shape throughout the relaxation as has been discussed by Anderson and Shuler (Reference 13).

Further, the consequences of anisotropic scattering on the relaxation rates can be seen qualitatively by writing out eqs. (13) and (14) with a general form for the collision operator,

18

$$\frac{\partial f_0}{\partial Nt} = \frac{1}{v^2} \frac{m}{M} \frac{\partial}{\partial v} [v^4(Q_0^0 - Q_1^0) f_0] \qquad (17)$$

$$\frac{\partial f_i}{\partial Nt} = -(Q_0^0 - Q_i^0) v f_i + \frac{m}{M}\frac{1}{v^2} \frac{\partial}{\partial v} [v^4(Q_0^0 - Q_i^0) f_i] \qquad (18)$$

$$\cong (Q_0^0 - Q_i^0) v f_i.$$

The solutions of these equations are the same as for eqs. (13) and (14). Since for forward scattering the quantity $(Q_0^0 - Q_i^0)$ is less than Q_0^0, the relaxation of the Legendre components of the EEDF is slower when the forward anisotropies in the cross sections are considered.

The field-free relaxation of an initially steady-state distribution function towards the gas temperature, assumed to be zero, represents a severe test of the numerical procedures used in the computer code. Figure 1 shows the results of one such comparison for a constant cross section model. This figure compares the EEDF's at an instant in time, $Nt = 1.3 \times 10^{10}$ cm^{-3}sec, when the initial electron energy has dropped to less than 10% of its initial value. The initial EEDF was assumed to be that appropriate to a constant cross section model at 1 Td with an elastic cross section of 6.6×10^{-18} cm^2 and a mass ratio m/M=.1. The two-term approximation was used for both the analytical and numerical calculation. Two points are to be noted in this figure. First, the agreement between the two curves is quite good over several orders of magnitude. The analytical EEDF drops abruptly to exactly zero at a velocity of 5.6×10^7 cm/sec for this example. Second, the EEDF is not a monotonically decreasing function of velocity throughout the relaxation. Steady-state two-term EEDF's are monotonically decreasing functions of velocity, but this monotonic behavior is not typical of the transient EEDF's except for the constant collision frequency model.
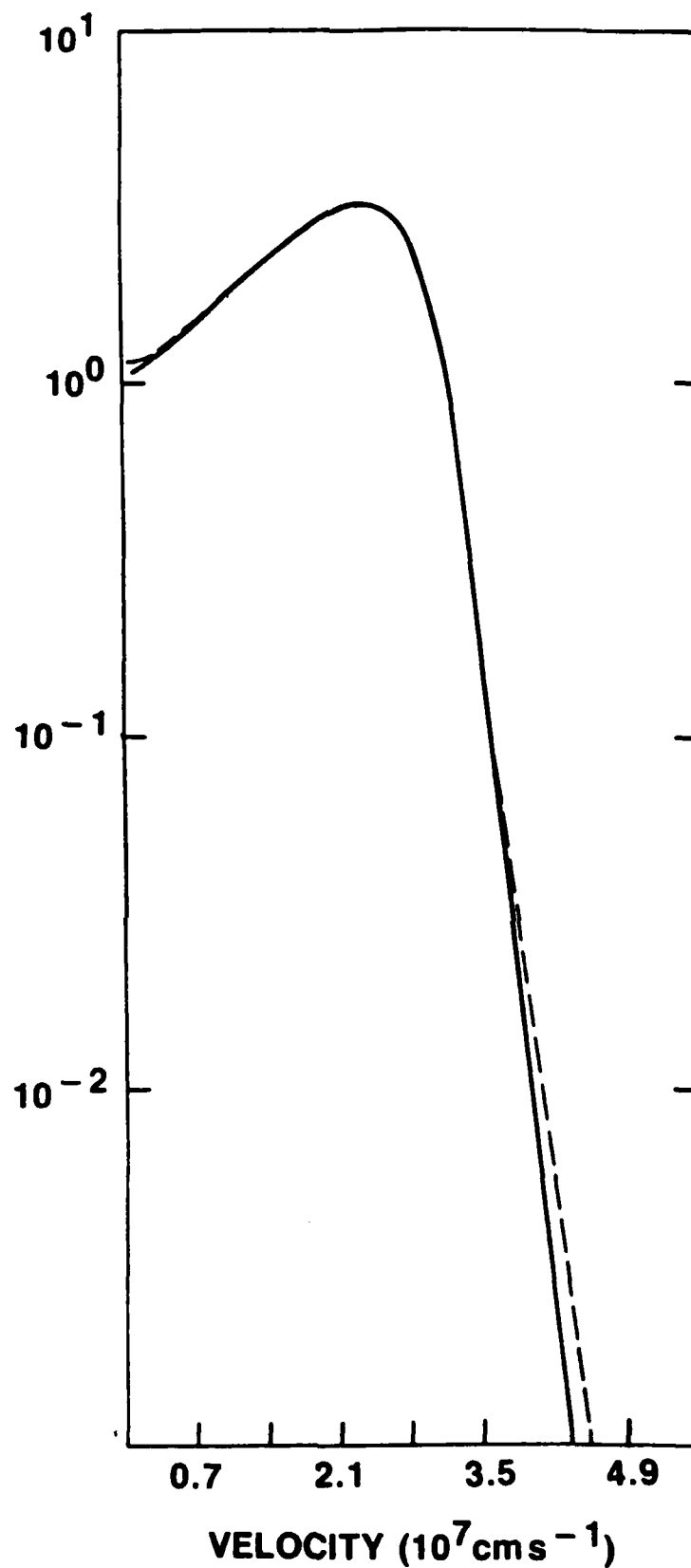
19

Figure 1. Isotropic EEDF for a constant cross section model at one instant in the field-free relaxation The dashed curve is the computer result and the solid curve is the analytical solution.

20

While the analytical results from this electron cooling model are primarily of theoretical interest, they were of considerable help in debugging the computer code. Simple models of the electron cooling problem have been discussed by several investigators, and in general we agree with the previous results.

2. Moment Equations with Finite Fields

The moment equations, velocity averages over the Boltzmann equation, have been widely used to describe electron transport for plasma (Reference 30) and solid-state (Reference 1) physics. A description of electron transport for weakly ionized gases based on the moment equations is less easy to implement, but nonetheless general. The continuity equation for electrons as given in eq. (4) is the 0th velocity moment of the Boltzmann equation and forms the basis for most models of gas discharges. If the coefficients in eq. (4) are known as functions of E/N and the gas composition, then eq.(4) provides a description of the time and space dependence of the electron density, and it is not necessary to find the solution for the distribution function from a kinetic (Boltzmann or Monte Carlo) model.

The general form of the velocity moments of the time-dependent Boltzmann eq. (7) can be written,

$$\frac{\partial V_i^n}{\partial Nt} = -\frac{a}{N} \frac{(i+1)}{(2i+3)} (n-i) V_{i+1}^{n-1} - \frac{a}{N} \frac{i}{(2i-1)} (n+i+1) V_{i-1}^{n-1}$$

$$+ \int v^{n+2} C[f_i] dv, \tag{19}$$

where we define the moments as speed and angle averages over the EEDF,

$$V_i^n (t) = \int v^n P_i (\cos\theta) f(\bar{v},t) d\bar{v} . \tag{20}$$

21

The first few moments are,

$$\frac{\partial ne}{\partial Nt} = \frac{\partial V^0_0}{\partial Nt} = \int v^2 C[f_0] \, dv \, , \tag{21a}$$

$$3\frac{\partial vd}{\partial Nt} = \frac{\partial V^1_1}{\partial Nt} = -3\frac{a}{N} V^0_0 + \int v^3 C[f_1] \, dv, \tag{21b}$$

$$\frac{\partial \langle v^2 \rangle}{\partial Nt} = \frac{\partial V^2_0}{\partial Nt} = -\frac{2a}{3N} V^1_1 + \int v^4 C[f_0] \, dv. \tag{21c}$$

These equations correspond physically to a spatially homogeneous or a spa-tially integrated description of an electron swarm and, hence, the 0th moment does not contain the spatial gradient terms seen in eq.(4).

There are two aspects of eqs.(21) that complicate the solution of the mo-ment equations. First, the form of the collision terms cannot be determined in general without knowledge of the EEDF. In some cases it is possible to ar-gue for a particular form of the EEDF and then to perform the integral numeri-cally (Reference 31). In highly ionized gases, for example, the EEDF is max-wellian. Another approach has been to parameterize the EEDF by one of the moments, the average energy (References 32, 33) or the average velocity, for example, and to solve the resulting coupled set of moment equations.

A second complication that occurs in the solution of the moment equations is that the moments are each coupled at most to the one higher and the one lower in angle through the field term and, depending on the energy dependence of the cross sections, to other speed moments through the collision terms. Some truncation of the set of equations must therefore be assumed. There are

22

certain established procedures for truncation of the moment equations for highly ionized gases (Reference 30) and this truncation can always be carried out at a higher order to assess the effect of the truncation empirically.

In many applications in gas discharge physics, we are also interested in determining the excitation rate coefficients. These can be determined in principle from a knowledge of all the moments; but, in practice, it is more convenient to return to a kinetic description for the calculation of excitation rate coefficients.

It is informative to look at solutions of the moment equations for certain model cases. If we assume a constant collision frequency and no ionization or attachment, rate equations for the moments can be written as

$$\frac{\partial V_0^0}{\partial Nt} \quad = \quad 0, \tag{22a}$$

$$\frac{\partial V_i^n}{\partial Nt} \quad = \quad - \frac{a}{N} \frac{(i+1)}{(2i+3)} (n-i) V_{i+1}^{n-1} - \frac{a}{N} \frac{i}{(2i-1)} (n+i+1) V_{i-1}^{n-1}$$

$$+ \nu V_i^n \quad , \quad i > 0. \tag{22b}$$

Although these forms for the moment equations are often assumed to be accurate in general, it is only for a constant collision frequency model that the collision integrals reduce to the simple analytical expressions given in the last terms of the RHS's of the equations above.

It is interesting to note here that the $i=n$ moments are coupled only to the lower moments. In particular, the drift velocity moment, $i=n=1$, depends only on the $i=n=0$ moment and is independent of how the moment equations are truncated. Independently of the cross section model, the drift velocity moment

is coupled to the higher order moments only through collision terms. This weak coupling explains why the drift velocity is so little affected by the two-term approximation compared to the average energy, for example. Further, in the collisionless limit, the drift velocity and average energy are given exactly by the two-term approximation because there is no coupling to the higher-order moments. The two-term EEDF's will be in error, but the drift and average energy moments will be exact.

When the acceleration due to the field in the constant collision frequency model is independent of time, the solutions of the i=n=0; i=n=1; and i=0,n=1 moments can be written,

$$n_e(t) = \text{Constant,} \tag{23a}$$

$$v_d(t) = \frac{a}{\nu} (e^{-\nu t} - 1) - v_d(t=o)e^{-\nu t}, \tag{23b}$$

$$\langle v^2 \rangle = B \exp(-2\frac{m}{M}\nu t) + A \exp(-\nu t) + \frac{a^2}{\nu^2}\frac{M}{m}. \tag{23c}$$

The electron density is constant in time because there are no electron creation or destruction mechanisms in this model. From eq.(23b) it can be seen that the difference between $v_d(t)$ and the final steady-state value of the drift velocity decays like $\exp(-\nu t)$ and the steady-state drift velocity is a/ν. In eq.(23c) above, A depends on the value of the drift velocity at t=0 and B is a function of the initial value of the average electron energy. The average electron energy approaches its steady-state value with two time constants. The term including $\exp(-\nu t)$ describes the coupling between the directed component of the velocity and the random velocity. The directed velocity is converted to random velocity after each collision. The longer time

constant in the term $\exp(-2(m/M)\nu t)$ represents an energy exchange frequency and describes how fast the electrons transfer energy to the neutrals due to elastic collisions and the associated recoil energy loss.

Solutions can also be found for the higher moments in the constant collision frequency model. In general the relaxation of the even, higher-order speed moments, V^{2n}_0, is a sum of terms with different time constants including terms up to $\exp(-2n(m/M)\nu t)$ where $n > M/2m$ is an analytical cut-off because no relaxation occurs faster than the collision time. Thus the even, higher-order speed moments equilibrate with the successively lower-order, even speed moments until they all follow the time dependence of the average energy. The slowest time constant is the energy exchange frequency, and at late times in the relaxation all the even-order speed moments relax with the average electron energy. When ionization is present, the slowest time constant will be the inverse of the ionization frequency and all moments will eventually relax like the electron density (Reference 23). The normalized moments V^n_i / V^0_0, will, however, be constant at late times.

If it is assumed that $\partial f_1 / \partial t = 0$ for $i>0$, or equivalently, that $\partial V^n_i / \partial t = 0$ for $i>0$, the only time dependence in the solutions of the moment equations will be $\exp(-2(m/M)\nu t)$ and an initial maxwellian will relax through a series of maxwellians to the steady-state EEDF. All previous Boltzmann calculations make this assumption (References 14, 18, 19) and it is valid for times $> \nu^{-1}$. At early times, the transient EEDF's are non-maxwellian; the deviation from a maxwellian at early times is due to the conversion of directed to random velocity. Because the directed velocity is usually a small fraction of the random velocity, the deviation from a maxwellian will be small. As the ratio of the energy exchange frequency to the momentum exchange frequency increases, the non-maxwellian region becomes correspondingly more important in the overall relaxation.

The implications of anisotropic scattering in the solutions of the moment equations are similar to those discussed for field-free case. If only elastic

recoil energy losses are considered, relaxation will be slower because the energy exchange will be slower. If inelastic processes are also considered, the energy exchange will be dominated by the inelastic processes and the anisotropic scattering will not appreciably affect the energy exchange frequency. It can, however, significantly affect the momentum exchange frequency and hence the validity of the usual approximation that $\partial f_i/\partial t=0$ for $i > 0$.

Solutions to the moment equations can also be found for time-dependent fields. If this constant collision frequency model is extended to the case of a time dependent acceleration of the form $a=a_0\cos(\omega t)$, the solutions of the $i=n=1$ moment equation can be written,

$$v_d(t) = v_d(t=0) \, e^{-\nu t} + \frac{a_0}{\nu} \, F_{eff} \, \cos[\omega t - \arccos F_{eff}] \qquad (24)$$

where,

$$F_{eff} = \left[\frac{\nu^2}{\nu^2 + \omega^2}\right]^{1/2} . \qquad (25)$$

From eq.(24) it can be seen that the instantaneous drift velocity differs by the factor F_{eff} from the value that would follow from the solution of eq.(22b) as given in eq.(23b) and using a local field approximation. There is also a phase shift given by the same factor F_{eff}. This phase shift describes how the current lags the applied voltage in an rf excited discharge in the region where the field is uniform and penetrates the body of the plasma.

The form of F_{eff} is identical to the modification of the field in the effective field treatment of rf EEDF's. The effective field concept was derived by Holstein (Reference 25) in 1946, and it is based on several approximations. The electrons gain energy, on the average, in an oscillating field only when they collide with the neutrals. The effective field concept models this by

26

replacing the cosine time dependence of the field with an effective average heating field. In his derivation of the effective field, Holstein assumed that the velocity derivative of the isotropic part of the EEDF changes very little over one cycle of the field. The usual two-term approximation, which replaces two partial differential equations with one second order ODE for f_0, depends on this approximation for AC fields (References 18, 19, 25). Also, in the usual two-term treatment of AC fields, since it is only the averages over one cycle of the field that are accessible, that treatment cannot resolve the phase shift between the drift velocity and the applied voltage. By following the time-dependence of the EEDF subjected to an rf field, it is possible to examine the validity of the effective field concept. Results from these comparisons in nitrogen will be discussed in Section IV.

It is not possible to solve the moment equations analytically for a more general collision model than the constant collision frequency model. For a cross section which depends on powers of the velocity greater than -1, the system of moment equations is further coupled through the collision terms. These are in principle numerically solvable, but it is just as easy to solve the Boltzmann equation. This coupling implies that the clean separation of time constants does not appear for any model other than the constant collision frequency case. This implication will be validated in the numerical results to follow.

3. Numerical Results in Finite Fields

In this section results of the numerical calculations of the time-dependent EEDF using the computer code described above are presented. The results are first shown for the model cases where we have analytical results are available for comparison.

a. Constant Collision Frequency

27

Figure 2 shows the isotropic part of the EEDF for a constant collision frequency model when the field is suddenly decreased. The initial (1 Td) and final (.5 Td) EEDF's are shown along with three at intermediate times. The normalized collision frequency ν/N in this example was 5.93×10^{-9} cm^3/sec. The time-dependence of the drift velocity and average electron energy from the numerical calculations agree exactly with the analysis from the moment equations. The drift velocity drops very quickly to its final, steady-state value and the average energy approaches its steady-state value more slowly. The exponential time constants for the drift velocity and average electron energy are $(\nu)^{-1}$ and $(2(m/M)\nu)^{-1}$, respectively. The deviation from a maxwellian EEDF at the early times is too small to be resolved on the scale of Fig. 2.

The isotropic part of the EEDF can be fit with an "apparent" E/N such that

$$f_o [v,t,E(t)/N] = f_o [v,t=0,(E(t)/N)_{app}]. \tag{26}$$

All the time-dependent speed averages over the distribution function after a short time can be found from a knowledge of the steady-state averages as functions of E/N using the parameterization in eq.(26). This apparent E/N, shown in Fig. 3 for the same model as in Fig. 2, represents an early attempt to describe the the transient behavior of the average properties of the EEDF from a knowledge of the steady-state of local field distributions. It is valid only for a constant collision frequency. In this parameterization, the electrons don't remember their history, but rather feel an apparent field that is greater than the instantaneous field.

b. Constant Cross Section

The constant collision frequency model is a very special limiting case whose transient behavior is not typical of more realistic models. A constant cross section model, while retaining the computational simplicity of the con-
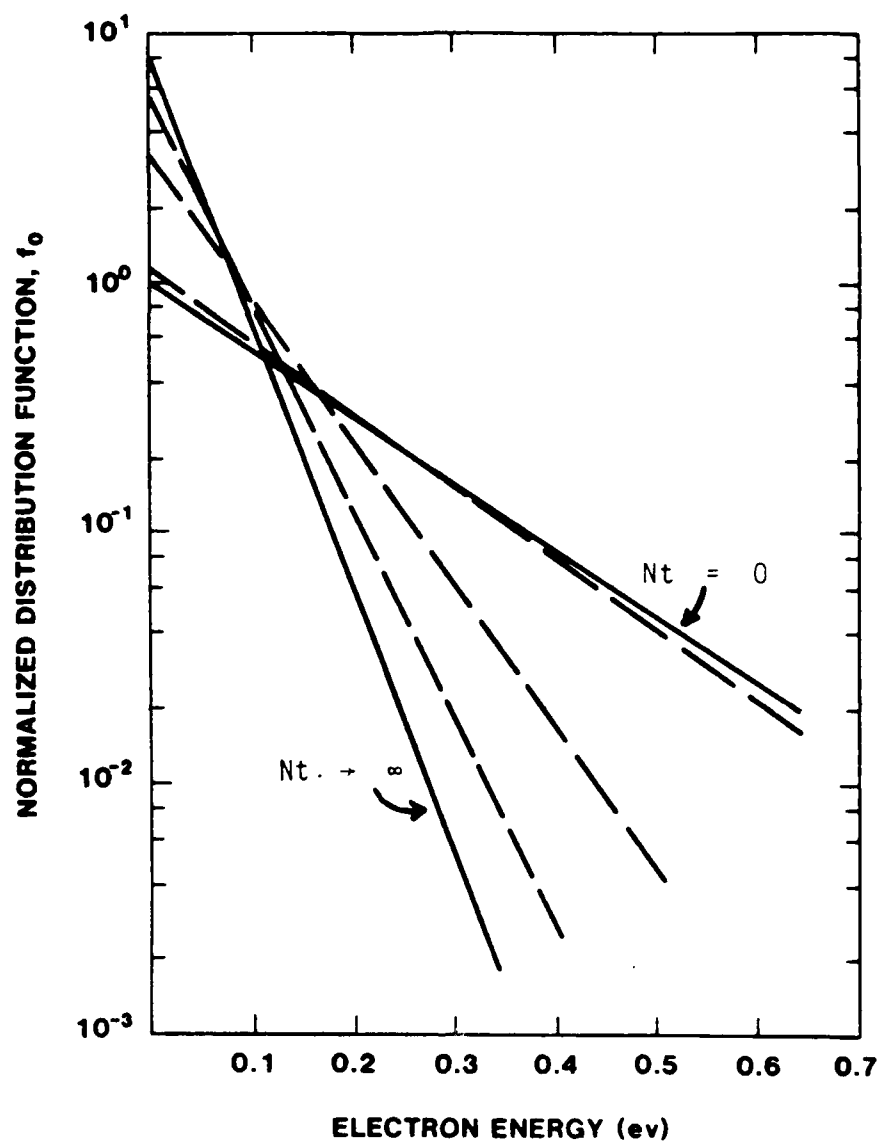
Figure 2. Isotropic EEDF relaxation for a constant collision frequency model. The initial EEDF is the steady-state EEDF at 1 Td and the E/N during relaxation is .5 Td.
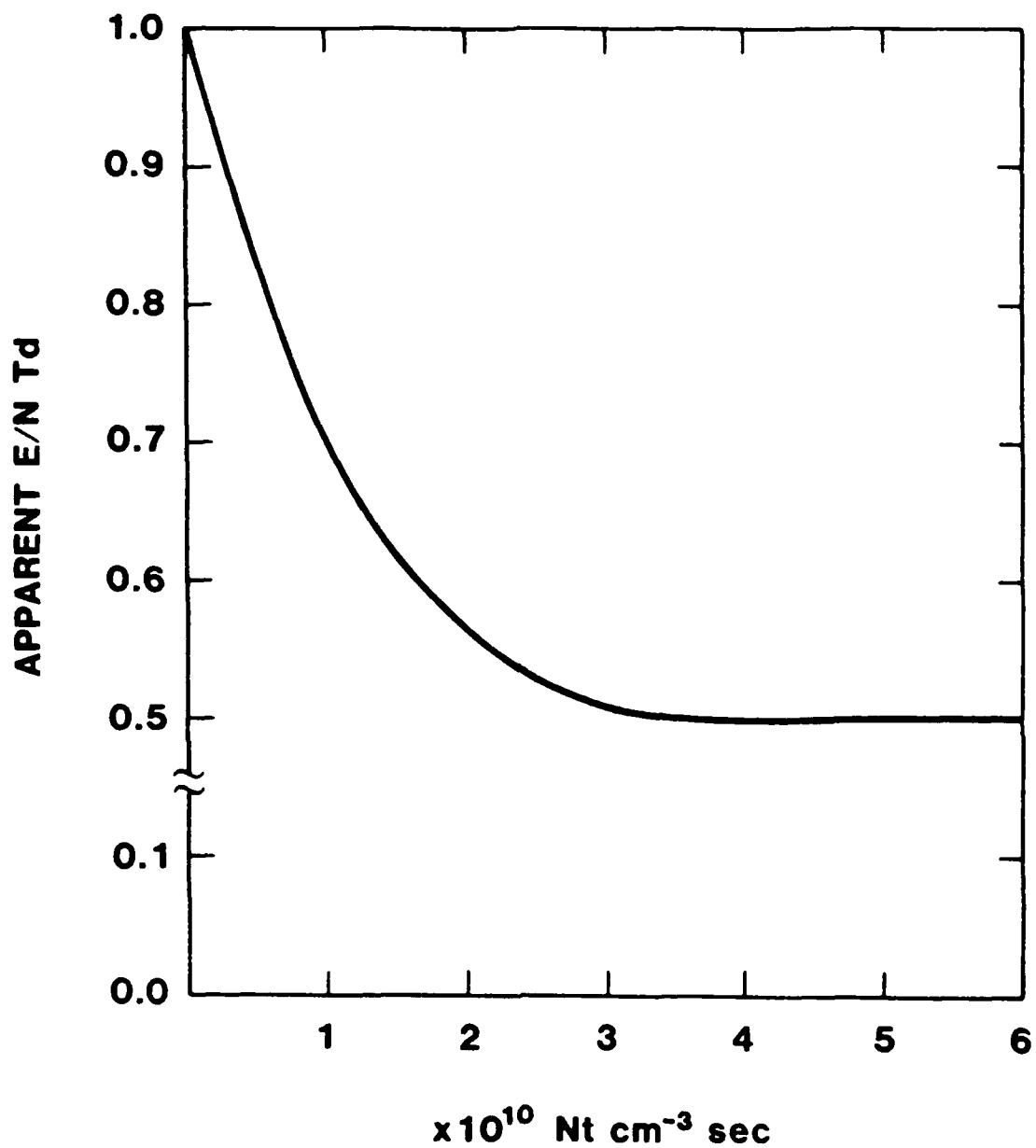
29

Figure 3. Apparent E/N during the relaxation in Fig. 2. The apparent E/N values were found by fitting the time-dependent EEDF's to the analytical form of the steady-state solution.

stant collision frequency model, illustrates all the transient phenomena seen
in the more detailed and realistic cross section models. The numerical values
for the parameters used in this model are;

$$Q = \text{constant} = 1 \times 10^{-16} \text{ cm}^2 \text{ ,}$$

$$m/M = .01 \text{ ,}$$

$$E(t=0)/N = 1 \text{ Td ,}$$

$$E(t>0)/N = .5 \text{ Td .}$$

Figure 4 shows the transition of the isotropic part of the EEDF from a
steady-state at 1 Td to a steady-state at .5 Td. The derivative $\partial f_0(v=0)/\partial v$
is > 0 for the transient distribution. In the steady-state two-term approxi-
mation, that derivative is identically zero. The positive derivative at $v = 0$
in the steady-state two-term approximation implies a changing sign in f_1. (We
find a nonzero derivative at zero in general in the steady-state multi-term
solutions, but this only implies a changing sign of f_1 in the two-term approx-
imation.)

Several interesting features are seen in Fig. 5 which shows the relaxa-
tion of the f_1 component for the same model as in Fig. 4. The rapid collapse
of the momentum as the field is suddenly decreased can be seen clearly in the
left of the figure. The abrupt decrease in f_1 is easy to understand. In the
absence of a field, the electron momentum is lost after one collision (assum-
ing isotropic scattering), and when the field is suddenly decreased, the elec-
tron momentum gained between collisions is suddenly decreased. This is re-
flected after one collision in f_1. The subsequent build-up of the momentum as
the EEDF approaches the new steady-state is very much slower than the collapse
at early time and reflects the energy readjustment to steady-state.
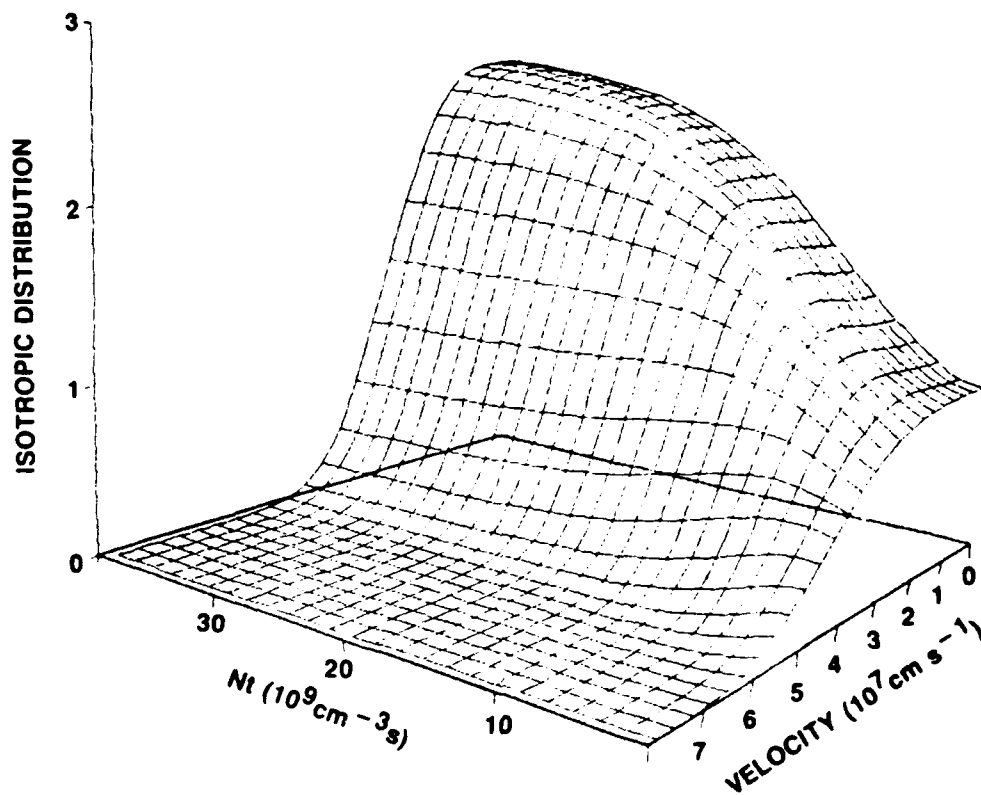
31

Figure 4. Isotropic EEDF relaxation for a constant cross section model. The initial EEDF is the steady-state EEDF at 1 Td and the E/N during relaxation is .5 Td.
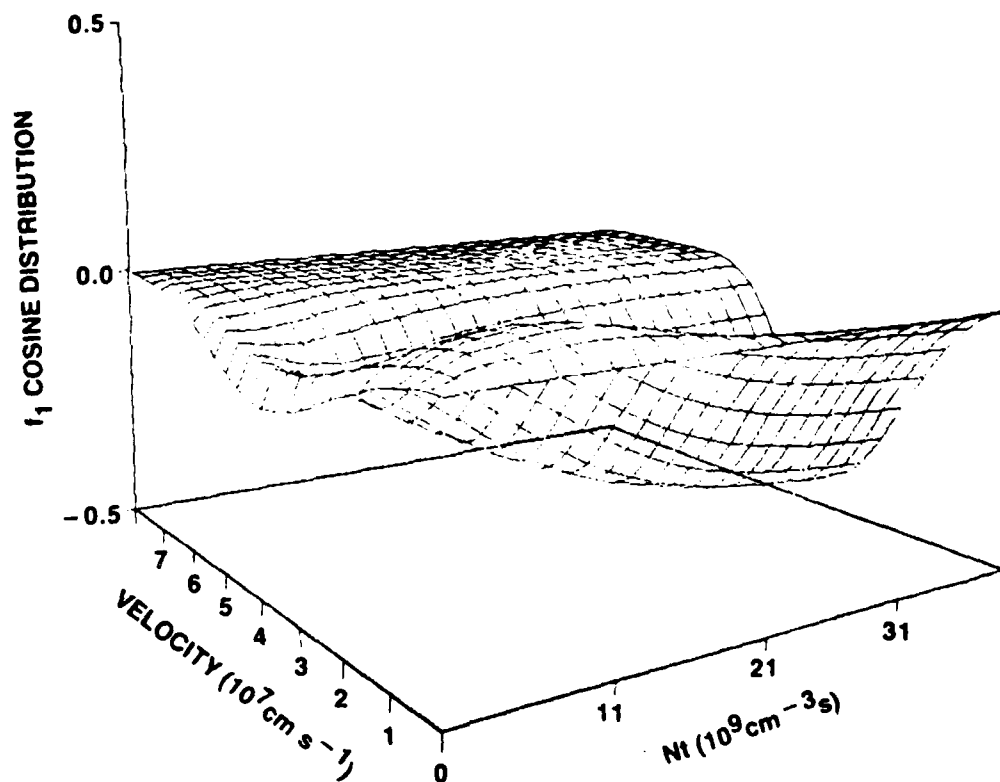
Figure 5. Anisotropic EEDF for the conditions of Fig. 4.

The changing sign of f_1 is coupled to the relaxation of the average electron energy and to the energy dependence of the collision frequency. The phenomenon is quite general and appears for all cases except a constant collision frequency when the field is decreased. When the field is suddenly reduced, the positive directed flux of high energy electrons will be rapidly attenuated due to collisions; the field will not be sufficient to maintain the flux of high energy electrons against the collisional retardation forces. The electrons comprising this flux will be redistributed uniformly in angle (assuming isotropic scattering) on lower velocity shells. On the other hand, the negative directed flux of high energy electrons will be attenuated to a lesser extent because these electrons stream against the field to lower total energies and into a region of decreasing collision frequency. Thus the rapid collisional depopulation of the high energy electrons reappears, in part, as a streaming-in source of the negative directed flux, and the net effect is an excess population of negative velocity electrons through the EEDF readjustment to the new field value. Cooling of the EEDF is thus effected not only by electrons colliding with the neutrals but also by electrons streaming against the field.

Figure 6 illustrates the behavior of the average energy and the drift velocity for the model in Figs. 4 and 5. In steady-state the collisional energy lost is balanced by the energy gained due to the field which is proportional to the drift velocity. The dashed line in the figure is ratio of the collional energy lost to E/N, R_c. This yields the collisional energy lost in units of the drift velocity (Reference 14), and when R_c is equal to the drift velocity, a steady-state has been reached. All three curves in the figure reach their steady-state values at approximately the same value of Nt, which is on the order of the inverse of the steady-state value of the energy exchange frequency.

The most striking feature appearing Fig. 6 is the undershoot in the drift velocity persisting until steady-state is reached. This undershoot occurs for all cases for when the field is decreased and when the electron mobility or
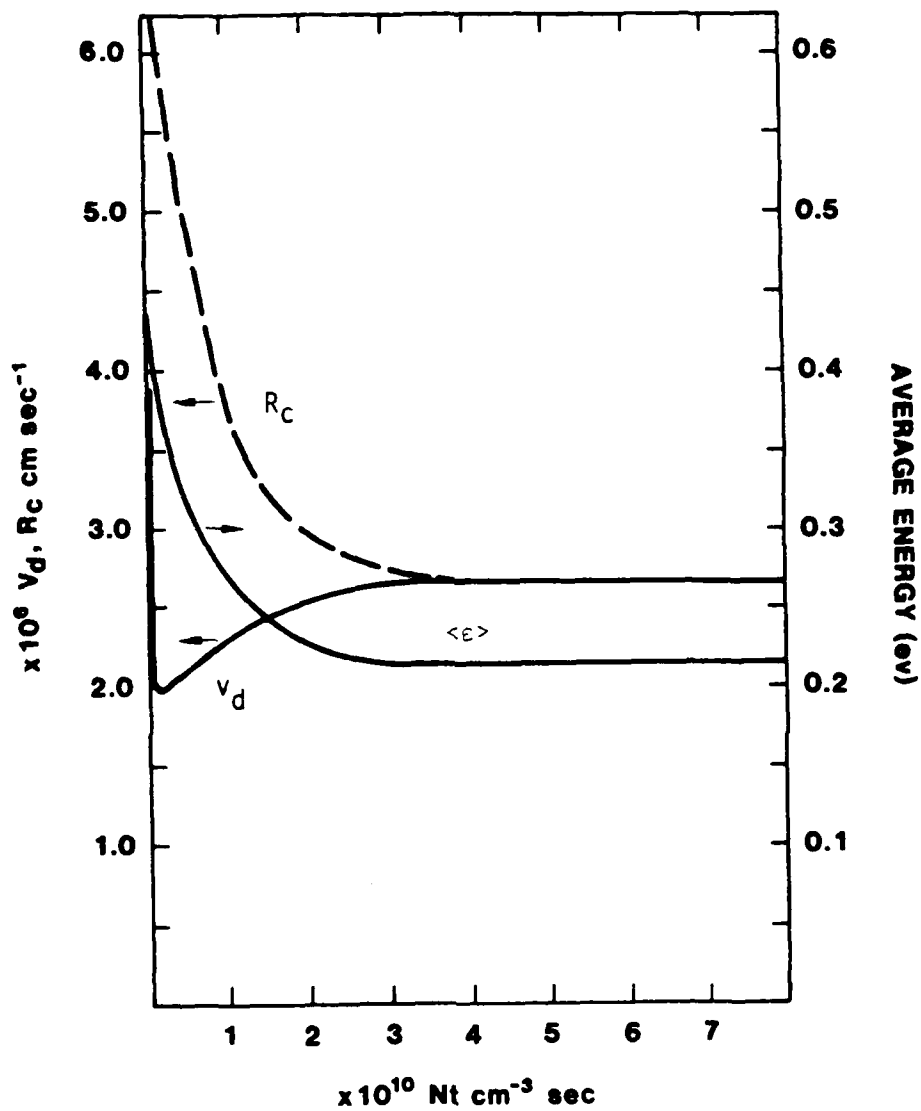
34

Figure 6.   Average energy, drift velocity and the ratio of the collisional power lost to E/N as functions of time for the conditions of Figs. 4 and 5.

35

collision frequency is a function of the electron energy. Until the energy relaxes to its lower, steady-state value, the mobility will continue to be too low. The electrons will experience too many collisions and the drift velocity will be correspondingly too low. It is clear why this effect is not seen for constant collision frequencies where electron mobility is independent of energy. The field cooling of a portion of the EEDF referred to above thus appears macroscopically as a reduced drift velocity or reduced power gained by the electrons from the field.

Although the models used in Figs. 1-6 include only elastic scattering, the large ratio of the electron to neutral mass has the effect of simulating inelastic processes and these models are expected to be indicative of transient phenomena in molecular gases.

c. Reid Model Atom

We turn now to a different model which includes one inelastic process – the Reid model atom (Reference 34). This model considers a constant elastic cross section of $6.\times10^{-16}$ cm^2 and an inelastic cross section with a threshold at .2 eV which increases linearly with energy. Figure 7 shows the relaxation of the drift velocity, average energy and excitation rate coefficient to a steady-state distribution at 24 Td for an inelastic cross section with a slope of $1.\times10^{-15}$ cm^2/eV above the threshold at .2 eV. The EEDF at t=0 was an isotropic maxwellian at a temperature of .176 eV. This figure shows the very different transient behaviors of the three average quantities. They all reach their steady-state value at about the same reduced time, $Nt \approx 3.5\times10^8$ cm^3/sec. Here an overshoot is seen in the drift velocity of about 30% with a slight secondary undershoot of about 4%. The average energy and the rate coefficient also display undershoots and overshoots but which are not nearly as pronounced as that in the drift velocity.

One of the purposes of this study is to determine the difference between the local field values of the transport and rate coefficients and their values
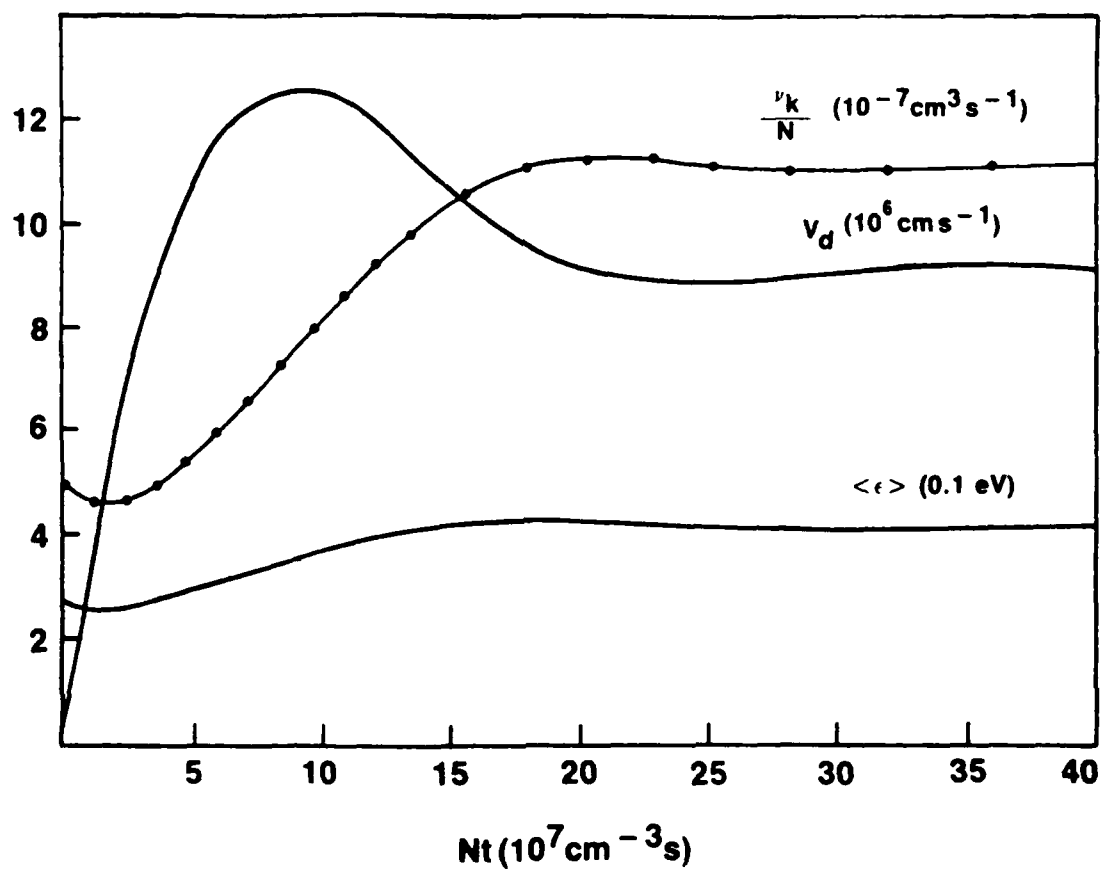
36

Figure 7. Average energy, drift velocity and excitation rate coefficient as functions of time for the Reid model atom at 24 Td. The initial EEDF is a maxwellian at a temperature of .176 eV and the inelastic cross section has a slope of 1.E-15 cm^2/eV.

calculated from the time-dependent Boltzmann equation, i.e., $v_d(E(t)/N)-v_d(t)$, where $v_d(E(t)/N)$ is the local field (the instantaneous field) value of the drift velocity. Figure 8 shows both values of the drift velocity as a function of Nt for the same model as in Fig. 7 but with an inelastic cross section of slope 2×10^{-16} cm^2/eV. The turn-on time of the field, also shown in the figure, is somewhat faster than the energy exchange time at steady-state (4.3×10^8 $cm^{-3}sec$) but slower than the momentum exchange time (1.8×10^7 $cm^{-3}sec$). It can be seen that the local value of the drift velocity differs from the calculated value by as much as 25%. The instantaneous field value is greater than $v_d(t)$ initially where the electrons are sluggish in responding to the field, but less than $v_d(t)$ in the region of the overshoot where the electron mobility is higher than its steady-state value. For this particular model, the time-dependent average energy is well approximated by the local field value primarily because the initial and steady-state values of the average energy do not differ greatly. The local field value of the rate coefficient is not a good approximation to the time-dependent value from the Boltzmann calculation. These results show the combined effects of the initial EEDF relaxation and the time-dependent field.

Figure 9 illustrates the effect of a finite turn-on time of the field on the overshoot in the drift velocity. The model parameters are the same as in Fig. 8. The field is turned-on exponentially as indicated in the figure. The drift velocity overshoot decreases from a maximum of 42% for a field which turns on faster than the momentum exchange time to a maximum of 15% for a field which turns on about twice as fast as the energy relaxes.

The isotropic and $\cos\theta$ components of the time-dependent EEDF's are shown in Figs. 10-17 for the Reid model atom as the model parameters are varied.

Figures 10 and 11 show the EEDF's corresponding to the $\beta=1 \times 10^{-6}$ cm^3/sec curve in Fig. 9. (The instability occurring at low velocities and at steady-state is due to numerical procedures which have since been improved to eliminate the oscillations. See Figs. 4-5.) The EEDF at t=0 was a maxwellian cor-
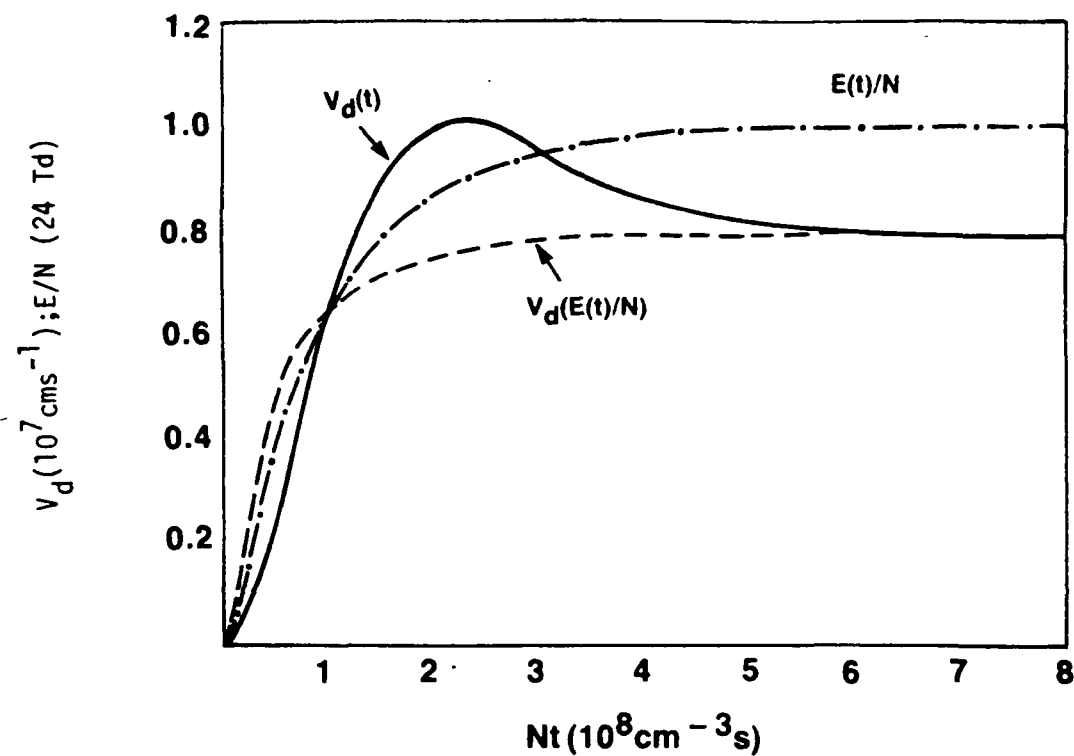
Figure 8. Comparision of the time-dependent drift velocity with the local field value for a time-dependent field. The conditions are as in Fig. 7 but with a slope of 2.E-16 cm^2/eV for the inelastic cross section.
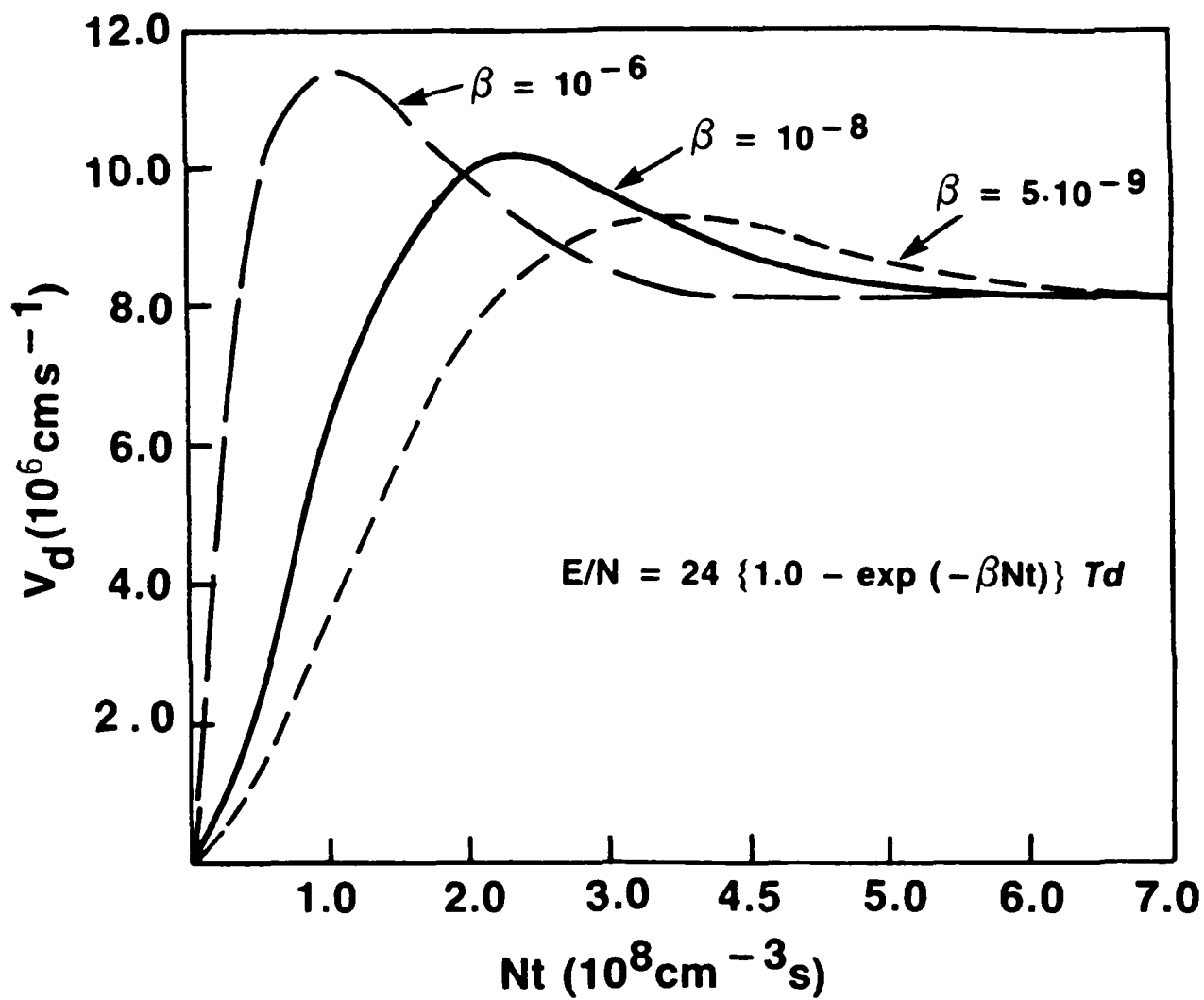
39

Figure 9. Time-dependent drift velocities for conditions as in Fig. 8 for three different time-dependent fields.
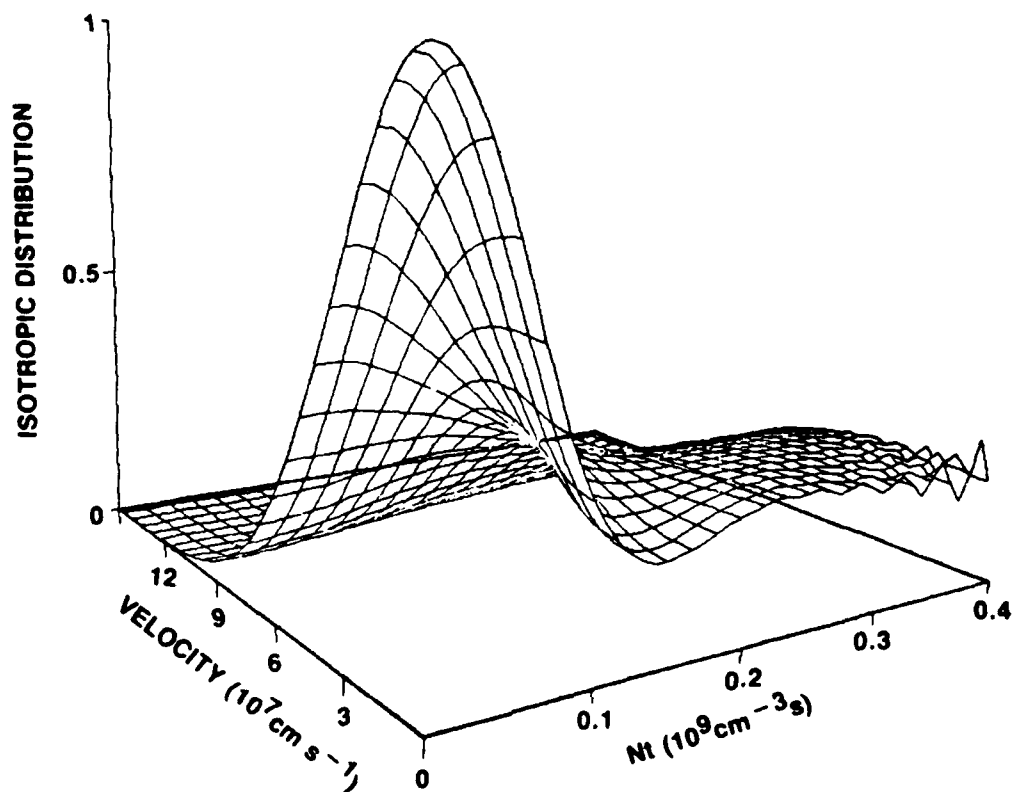
Figure 10. Time-dependent isotropic EEDF for conditions as in Fig. 9 and $\beta=1.E-06\ cm^3/sec$.

41
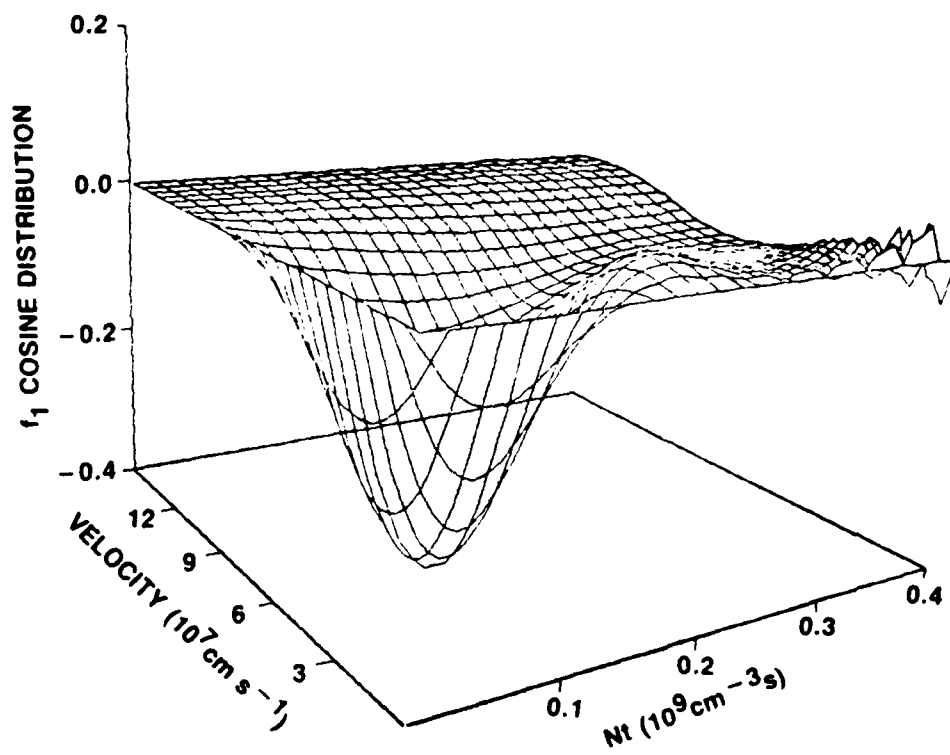
Figure 11. Time-dependent anisotropic EEDF corresponding to Fig. 10.

responding to an average electron energy of about .33 eV. The negative slope in f_0 at low velocities corresponds to the region of positive f_1. This cathode-directed component of the current is the same effect that was seen in the EEDF relaxation in Fig. 5. Note that the inelastic cross section threshold corresponds to 2.65×10^7 cm/sec.

As the frequency for the turn-on of the field is lowered to $\beta = 1 \times 10^{-8}$ cm^3/sec, the relaxation of the EEDF's seen in Figs. 12 and 13 is smoother, the cathode-directed current component almost disappears. Figs. 14 and 15 show the EEDF relaxation for $\beta = 1 \times 10^{-6}$ cm^3/sec as in Figs. 10 and 11 but the slope of the cross section was increased a factor of four to 8×10^{-16} cm^2/eV. The relaxation is faster, as would be expected on the basis of the moment arguments. In the region of positive f_1, the magnitude of f_1 is increased; the cathode-directed current component is enhanced. This behavior is consistent with the picture described above for the existence of the phenomena.

Another parameter that was varied in these model calculations was the average energy of the initial maxwellian. In Figs. 16 and 17 the relaxation of the EEDF is shown for the same model parameters as in Figs. 10 and 11 but with an initial average energy of .65 eV. (Note the change in the view angle in Fig. 16.) The final average electron energy is .85 eV for these parameters. The cathode-directed current component is again enhanced. This is at first surprising since the initial and final average energies are closer. However, for the same average electron energy, a maxwellian initial EEDF has more high energy electrons than does the EEDF for this model. Because of the increasing collision frequency with increasing energy, the collisional redistribution of electrons is faster and hence the negative directed flux is increased. Thus, the cathode-directed current component is enhanced.

A final parameter varied in these model studies was the field frequency. The full time dependence of the field $E = E_0 \cos((\omega/N)Nt)$ was included in these calculations for the Reid model atom with an inelastic cross section of slope 2×10^{-16} cm^2/eV. An effective field model is often used to model rf exctita-
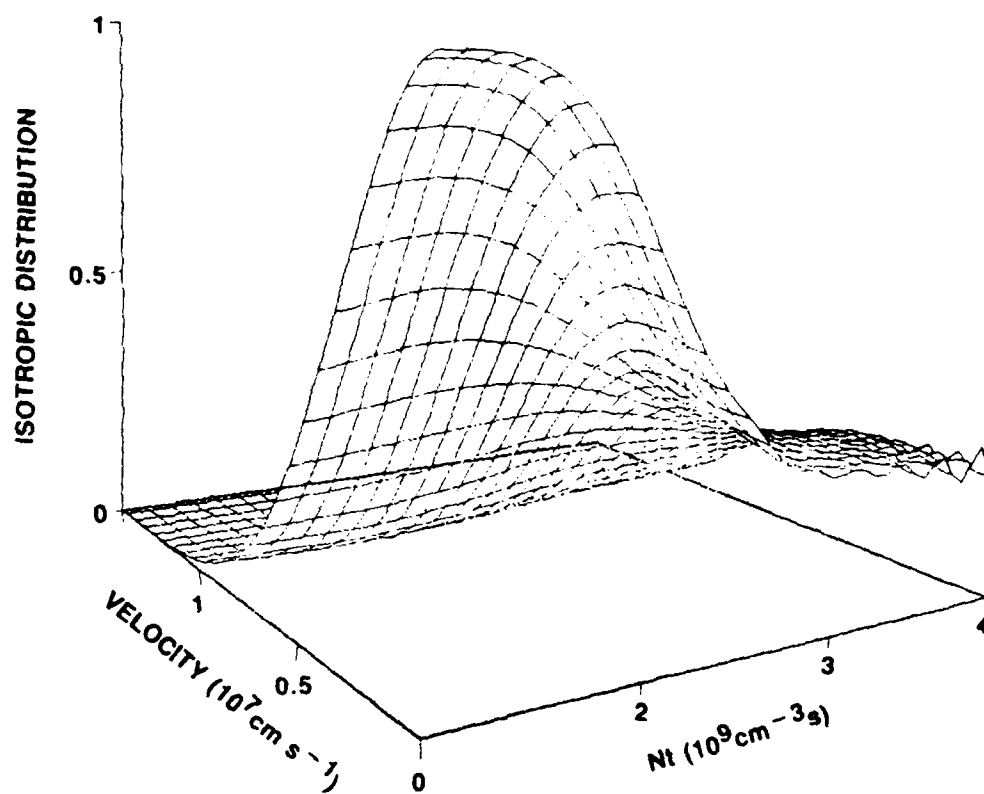
Figure 12. Time-dependent isotropic EEDF for conditions as in Fig. 9 and $\beta=1.E-08$ cm^3/sec.

44

Figure 13. Time-dependent anisotropic EEDF corresponding to Fig. 12.

Figure 14. Time-dependent isotropic EEDF for conditions as in Fig. 10, but with an inelastic cross section slope of 8.E-16 cm^2/eV.
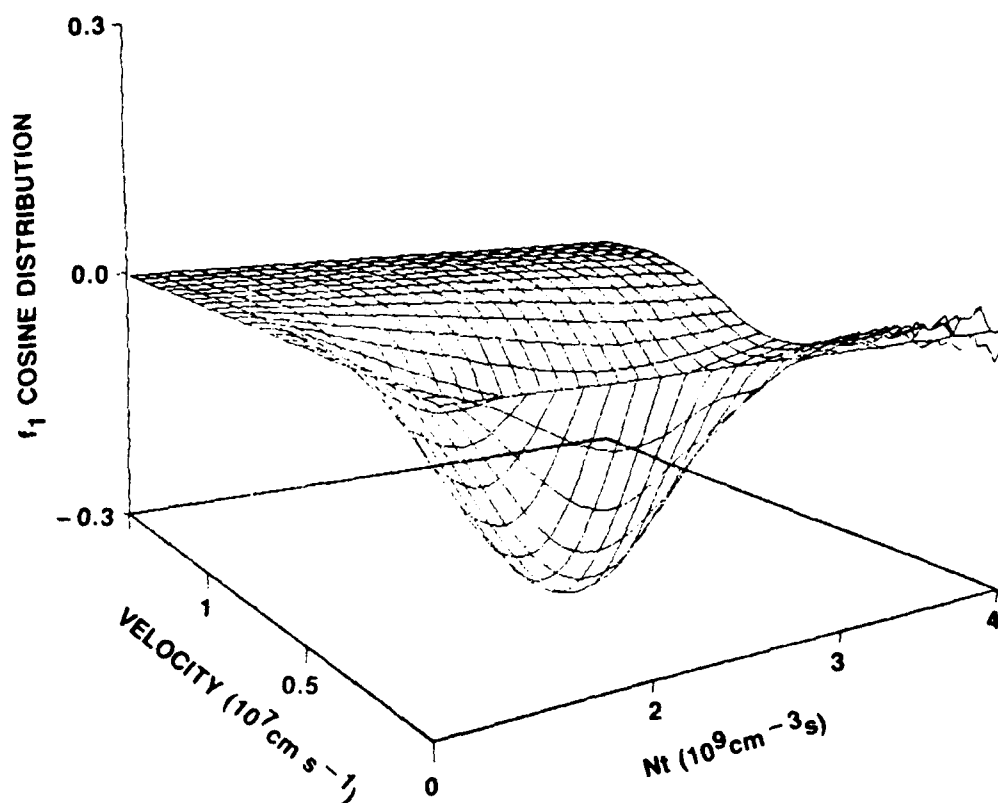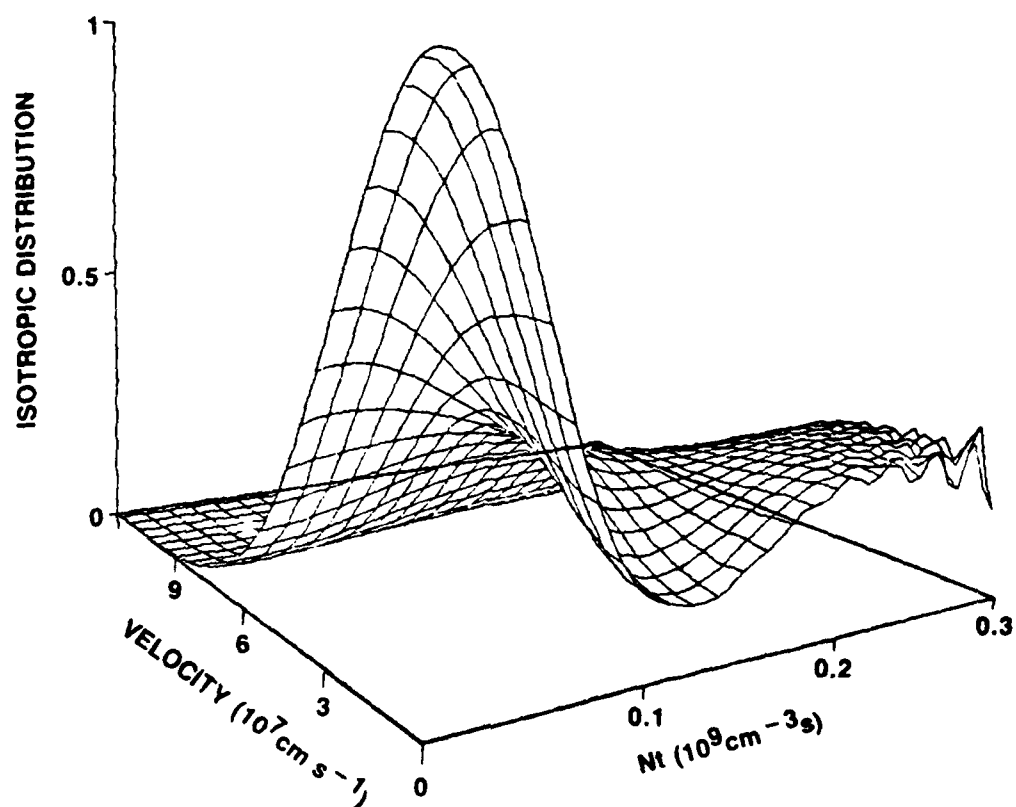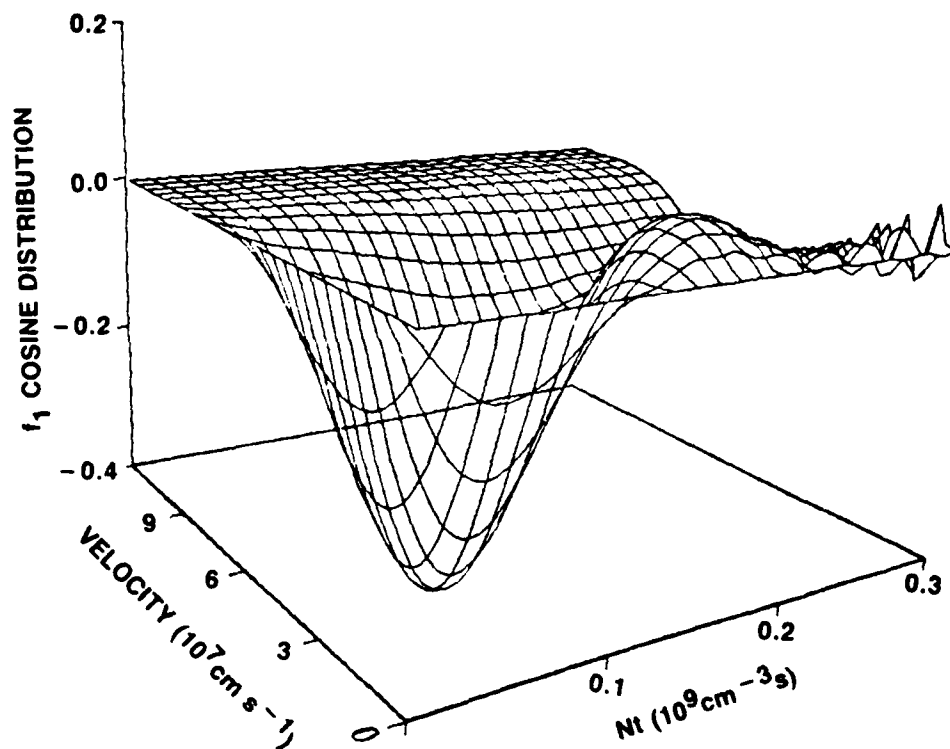
46

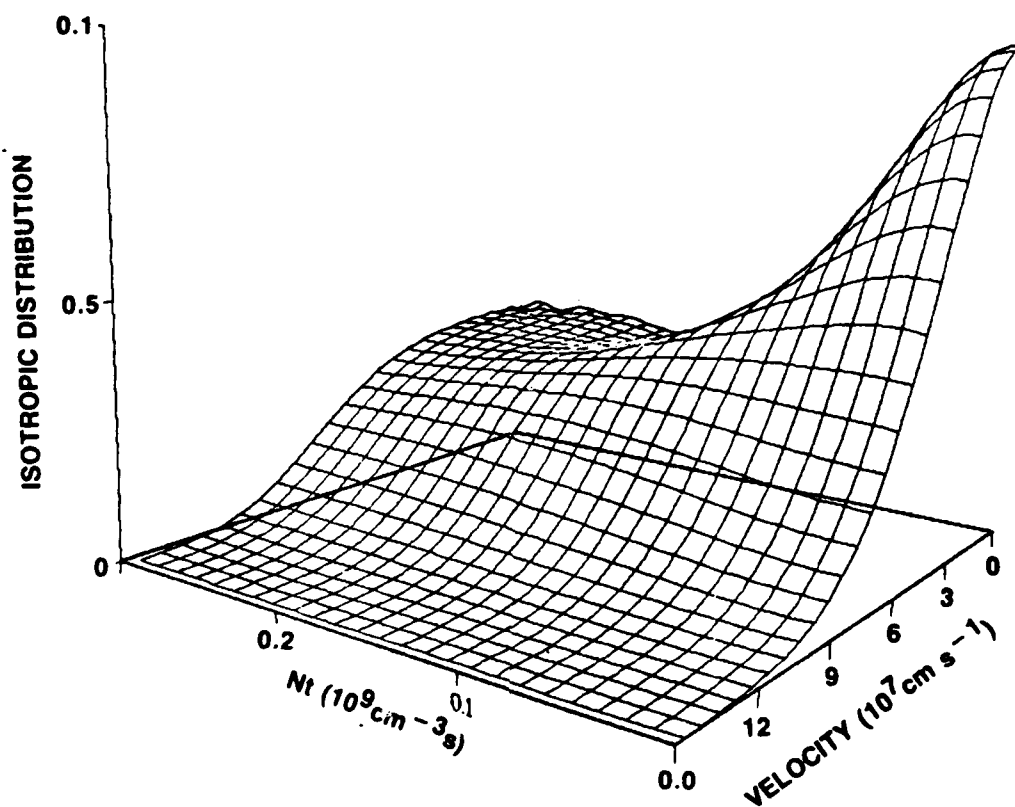Figure 15. Time-dependent anisotropic EEDF corresponding to Fig. 14.

47

Figure 16. Time-dependent isotropic EEDF for conditions as in Fig. 10, but with an intial electron average energy of .65 eV.
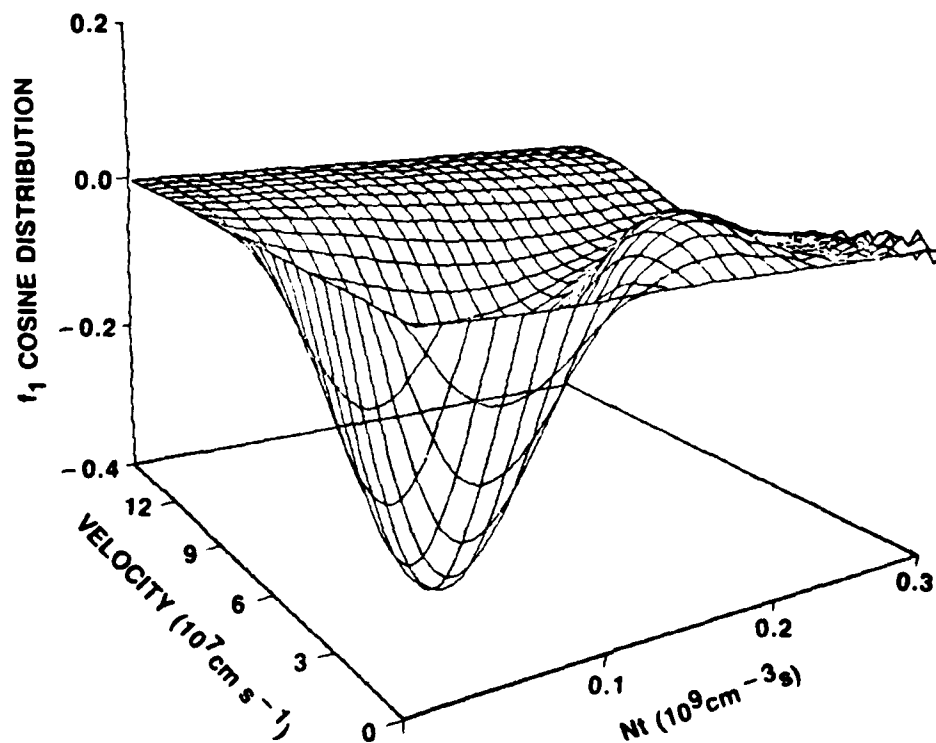
48

Figure 17. Time-dependent anisotropic EEDF corresponding to Fig. 16.

tion. As discussed after eq.(24), the form of the effective field was derived by Holstein by averaging the Boltzmann equation over one cycle of the field yielding a coefficient which multiplies the factor E/N,

$$\left(\frac{E}{N}\right)_{eff} = \left(\frac{E}{N}\right)_{rms} \left[\frac{\nu^2}{\nu^2 + \omega^2}\right]^{1/2} \tag{27}$$

where the ν's are velocity dependent. This form has been used in previous calculations of rf excitation . Often, however, an effective ν independent of velocity is used in eq.(27) to allow a simple scaling from dc to rf results. When the ν's are independent of velocity, the scaling is exact as was seen in the discussion of the moment equations. Figure 18 shows the normalized colli- sion frequency as a function of velocity for the model atom here. It is far from constant and difficult to estimate an "effective" constant collision fre- quency.

The full time dependence of the field for the calculations is retained here. However, unless the applications demand the detail of a full time-de- pendent calculation, we find it is appropriate to use the field in the form of eq.(27) provided that the velocity dependence of the collision frequency is explicitly included and provided the field does not oscillate significantly faster than the energy exchange. That is, averages of quantities over one cy- cle of the field compare well with the calculations using the field as given in eq.(27). Recall that the derivation leading to eq.(27) is particular to the two-term approximation and is only valid to that order. In the case that the energy exchange is faster than the field frequency, the EEDF can keep up with the oscillations in the field and a local field approximation with a slowly varying field should be used.

Figures 19-21 show the isotropic part of the EEDF for three different field frequencies. These frequencies are indicated in Fig. 18 for comparison with the collision frequency. The calculations are not shown through the full

50
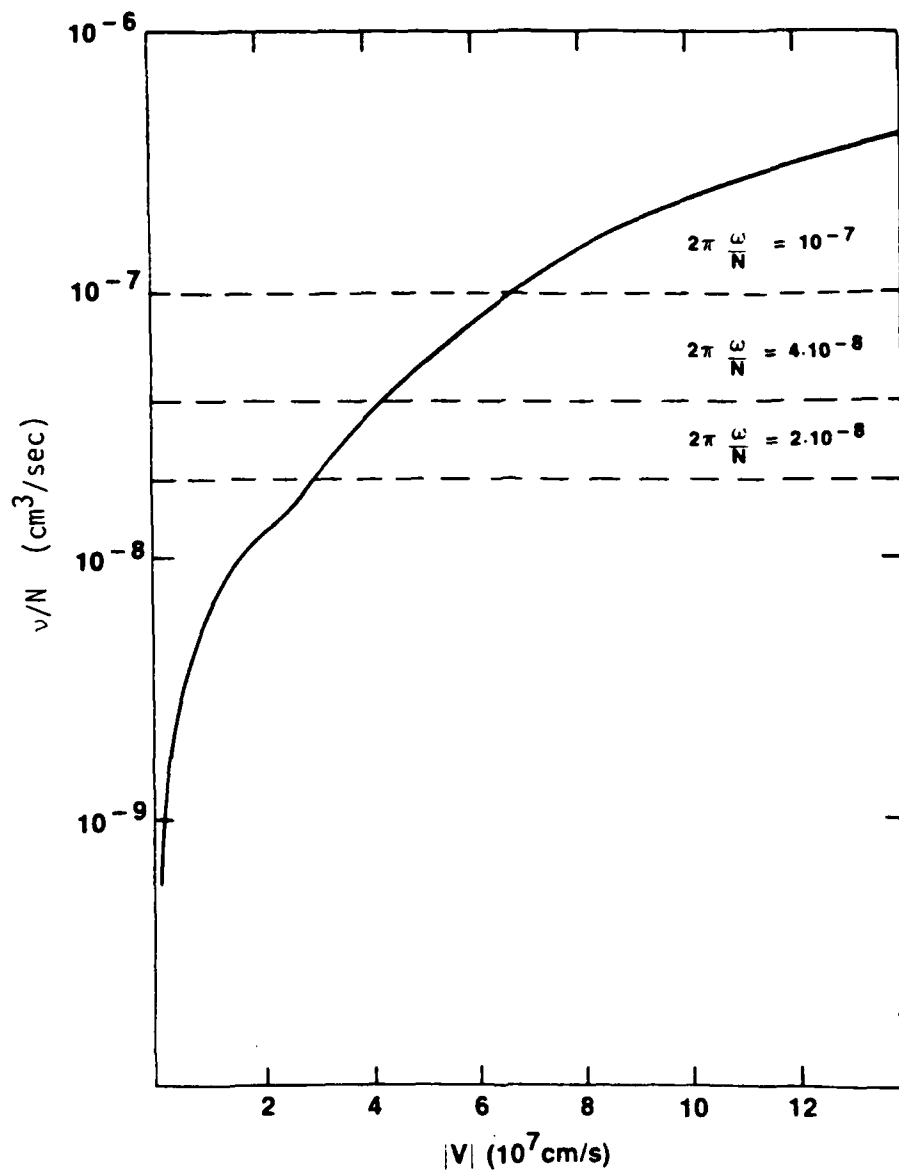
Figure 18. Normalized collision frequency, ν/N as a function of electron speed for an inelastic cross section slope of 2.E-16 cm^2/eV.
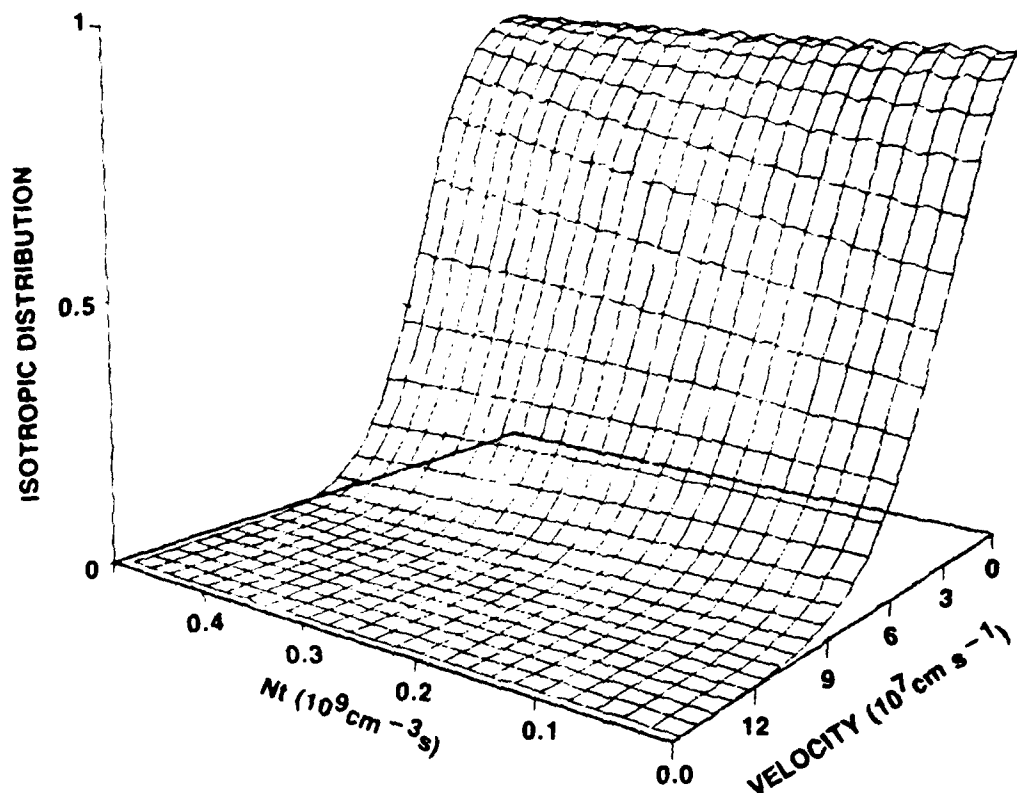
Figure 19. Time-dependent isotropic EEDF for rf excitation. The computation model is the Reid atom with an inelastic cross section slope of 2.E-16 cm^2/eV, and E/N of 24 Td. The normalized field frequency. ω/N is is 1.E-07 cm^3/sec.
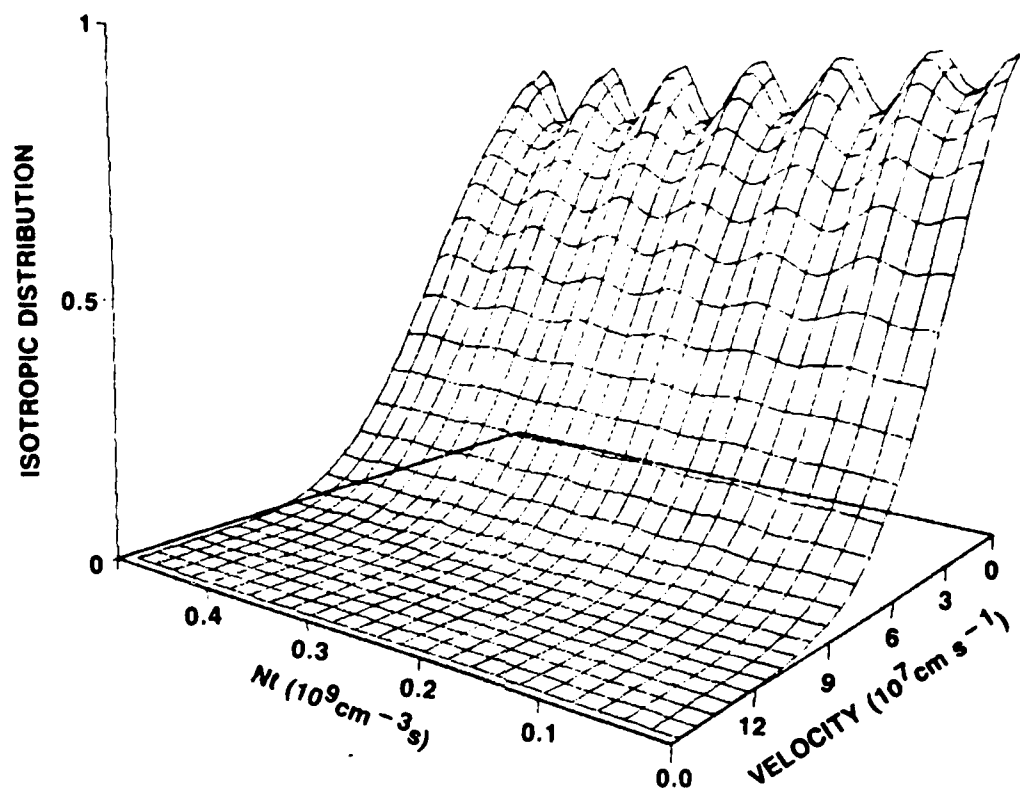
Figure 20. Same as Fig. 19 but with a normalized field frequency of 4.E-08 cm^3/sec.
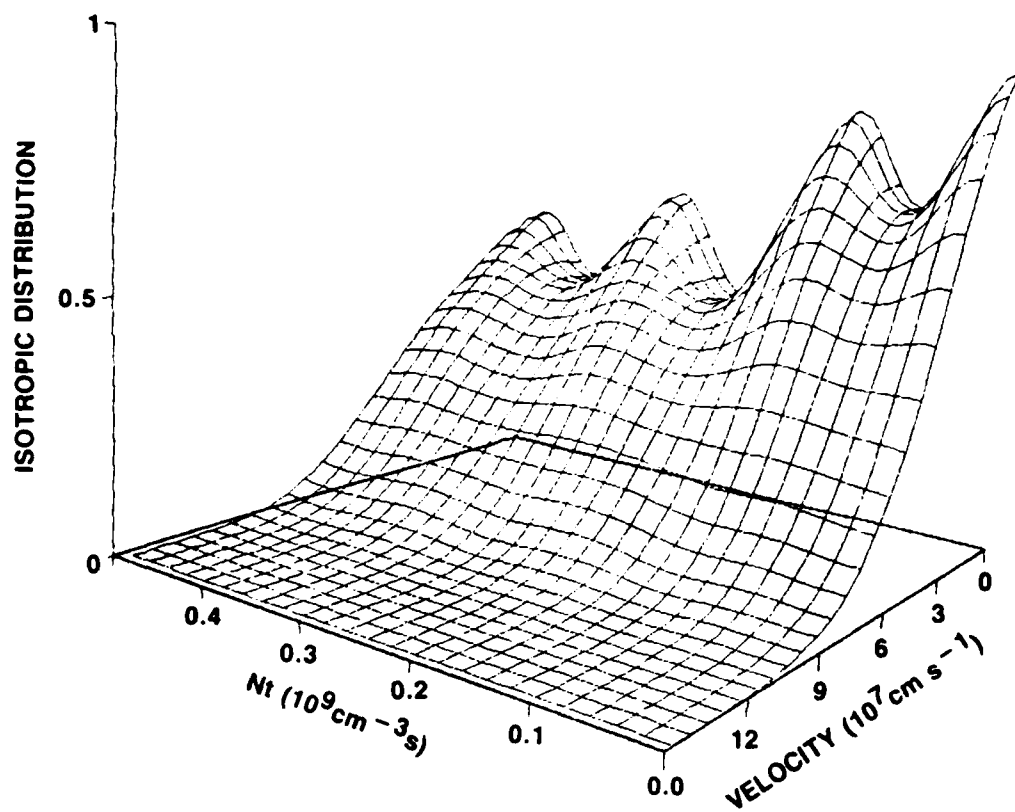
Figure 21. Same as for Fig. 19 but with a normalized field frequency of 2 E-09 cm^3 sec.

relaxation, but the figures illustrate the response of the EEDF to different field frequencies. For comparison, steady-state inelastic rate coefficients are 1.5×10^{-8}, 2.8×10^{-8} and 4.5×10^{-8} cm^3/sec for the normalized field frequencies, ω/N, of 1×10^{-7}, 4×10^{-8} and 2×10^{-8} cm^3/sec, respectively. Since it is not possible a priori to estimate the proper collision frequency for use with the standard effective field model, we make no attempt to compare.

To conclude, in these model studies we have used comparisons with analytical results to guide the development of the numerical methods used in the time-dependent Boltzmann calculations. The code has performed well for a variety of strenuous tests and we have confidence in the accuracy of the results. In the constant cross section model and the Reid model atom, we find examples of all the transient phenomena seen in the more detailed calculations using realistic cross sections. Differences between these results and the nitrogen results to be presented below are in detail only.

IV. Calculations in Nitrogen

Time-dependent Boltzmann calculations have been performed in nitrogen for a realistic but simplified set of cross sections (Reference 35). These cross sections are shown in Fig. 22. Four excitation levels are considered; effective vibrational, triplet and singlet excitation and ionization. Time-independent calculations using this set of cross sections have demonstrated that they yield rate and transport coefficients within 10% of the values obtained using a full set of 24 inelastic cross sections for E/N greater than 100 Td (Reference 35). This set of cross sections considerable reduces the computational times while retaining the essence of the physics for average electron energies greater than about 2 eV, the peak in the vibrational cross sections. New electrons born in the ionization events are included in these calculations, and the electrons exiting the ionization event are assumed to share equally the excess energy of the primary over the ionization potential. All cross sections are isotropic.

The results of the time-dependent calculations in nitrogen showed no new features beyond those already discussed from the model calculations. The detailed structure of the relaxation of the transport and rate coefficients differs from model to model but the same effects of drift velocity overshoots, undershoot, cathode-directed current components and nonmonotonic relaxation of the transport and rate coefficients appear in the nitrogen calculations as well.

Although the transport and rate coefficients relax with different time dependences, the steady-state values are all reached at about the same time. At low E/N where ionization is not very important, that time correlates with the energy relaxation time, more or less independently of the initial conditions. Relaxation is complete in most cases by $Nt = .5$ to 1.0×10^8 cm^{-3}sec for $E/N < 300$ Td. Thus for pressures greater than several torr, the relaxation is subnanosecond. At lower pressures, the transient effects persist to times long enough that they may be important in certain applications.
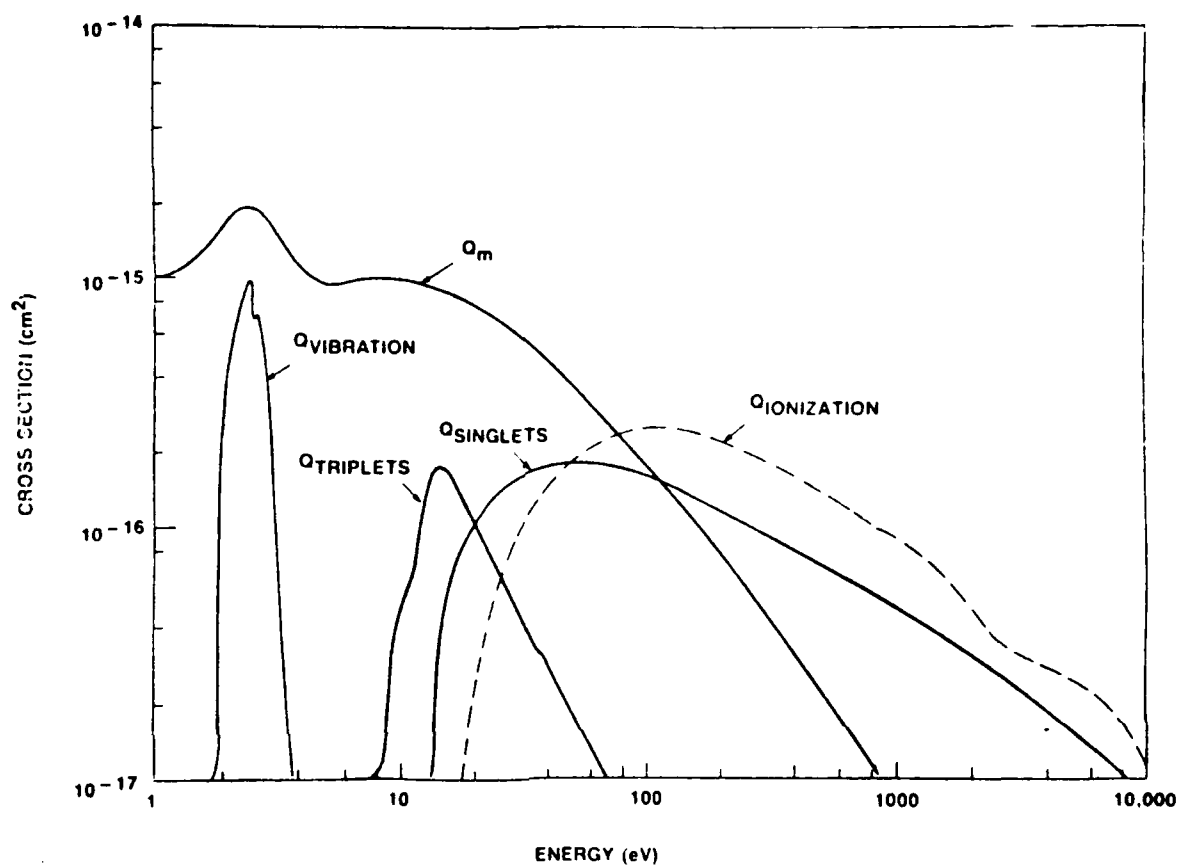
Figure 22.   Simplified set of cross sections used in the nitrogen calcula-
tions.

At the higher values of E/N, ionization occurs very rapidly and is very efficient at equilibrating the electron energies. Figure 23 shows the relaxation of the ionization rate coefficient, the average energy and the drift velocity at 3000 Td. The relaxation of these parameters is complete by 2.5×10^7 cm^{-3}sec, or by .7 nsec at 1 torr. Because the ionization frequency saturates at high E/N, there is an upper limit to the speed of the relaxation. The upper limit on the ionization rate is 1.9×10^{-7} cm^{-3}sec from the cross section data of Rapp and Englander-Golden (Reference 36).

In the course of this work an interesting application of these types of calculations came up in the context of the propogation of high-power, fast-rising microwave pulses through the atmosphere. In contrast to the DC examples shown above, the microwave EEDF's and all averages over the EEDF depend not only on E/N, but also on the field frequency. Figure 24 illustrates the regions of interest on an E/N versus E/ω diagram. The upper left corner is the high frequency limit where the only dependence is on E/ω (Reference 37), and the lower right corner is the DC limit where only E/N need be specified. The dots on the figure show where our calculations have been performed (Reference 38).

The AC calculations were done first using the full time dependence of the field, $E(t) = E_0 \cos(\omega t)$. The ionization rate and average energy were then found as averages over several cycles of the field after a quasi-steady-state was reached. Results from these calculations are shown in Fig. 25 as a function of E/ω for two different values of the ratio ω/N, appropriate to 35 GHz at 2.8 and 35 Torr. We can follow the turn-over in the ionization rate coefficient at high fields because electron runaway will not occur in a nonrelativistic treatment of an oscillating field, even though the average electron energies are extremely high. The highest field strength in these calculations was 4×10^5 V/cm at 35 GHz. To continue to even higher field strenghts would require a relativistic treatment and more cross section data
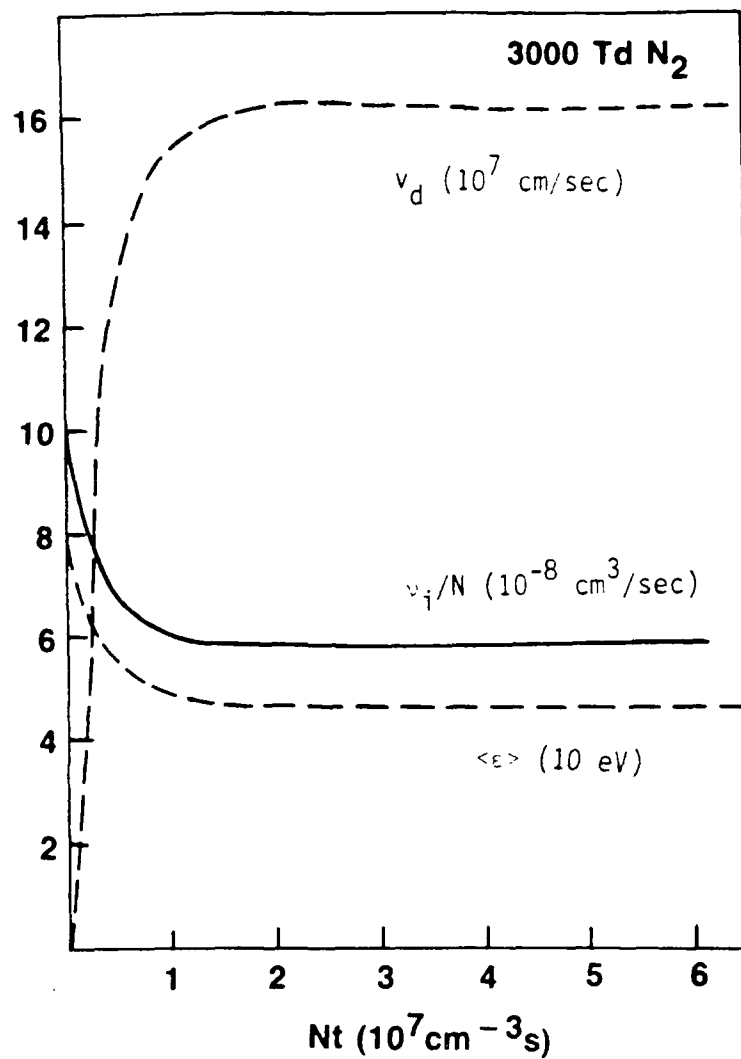
Figure 23. Time-dependent ionization rate coefficient, average electron energy and drift velocity in nitrogen at 3000 Td.
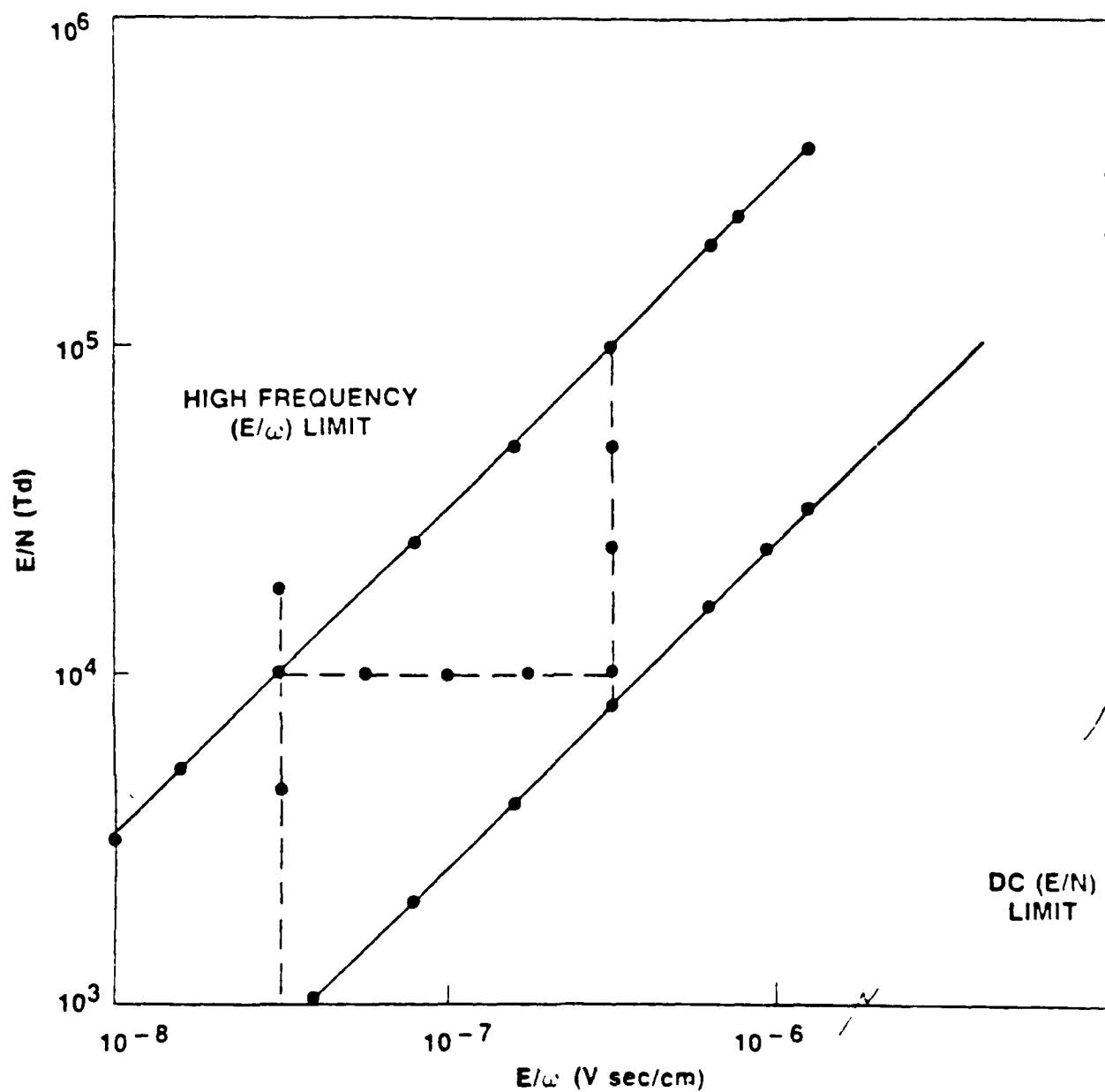
59

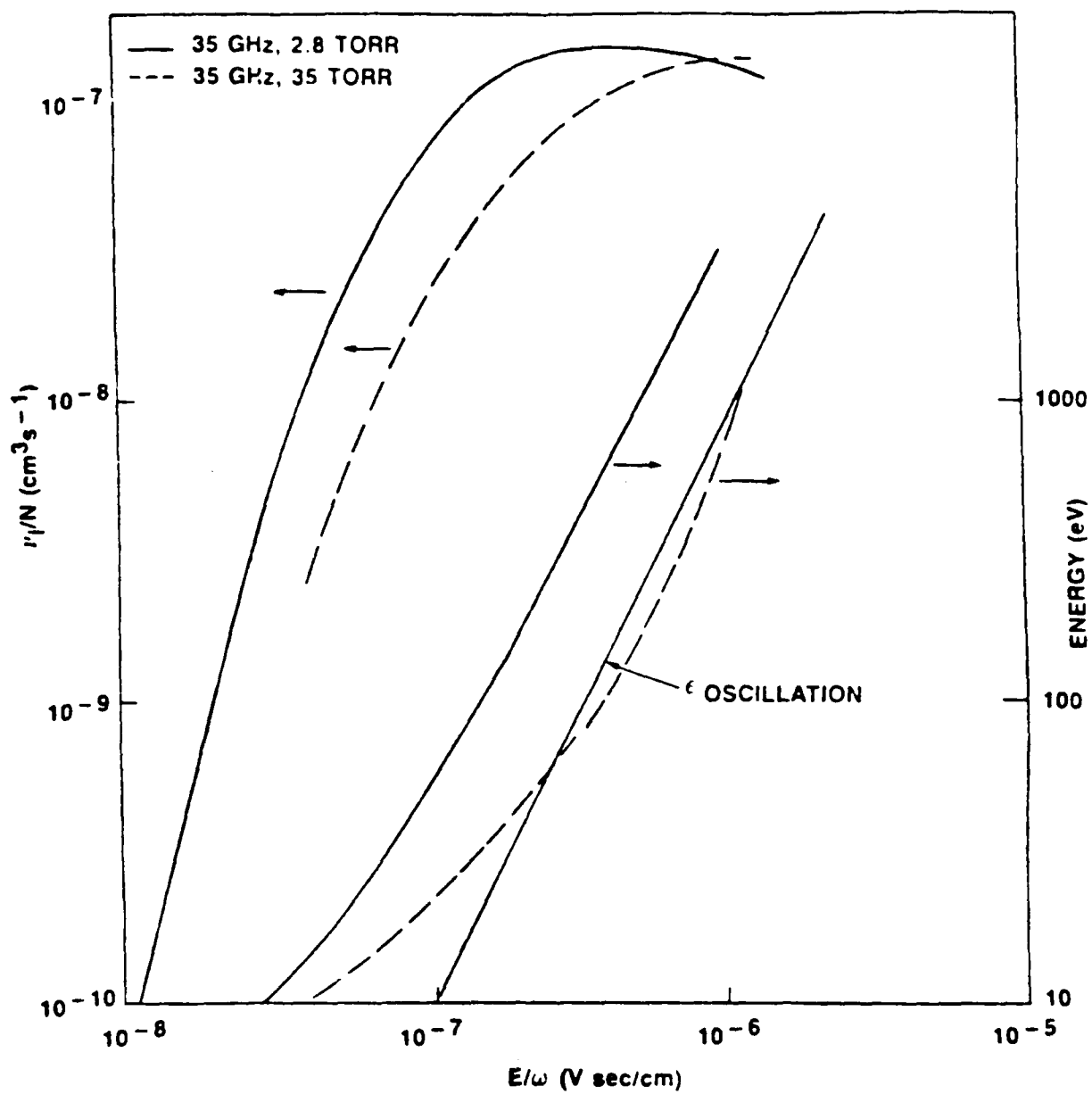Figure 24. E/N versus E/ω showing where the microwave calculations were performed.

60

Figure 25. Ionization rate coefficients and average electron energy as functions of E/ω for two different pressures at 35 GHz.

61

These calculations were also done using the velocity dependent form of the effective field (Reference 37) to compare with the full time-dependent calculations. We find that the velocity dependent effective field is good for values of the ratio of the field frequency to the collision frequency, ω/ν, less than two and for E/ω less than about $7. \times 10^{-7}$ Vsec/cm. At higher values of E/ω and for ω/ν greater than two, the effective field predicts electron runaway which does not occur in a nonrelativistic treatment of rf fields. Thus, the effective field in the form given in eq. (27) is not valid when the ionization rate is high. It should be possible to push the validity of the effective field to higher frequencies and higher E/ω if the ionization frequency were included in the collision frequency ($\nu \rightarrow \nu + \nu_i$), but this has not been tested. For a high E/ω and for ω/ν greater than about four, the results are independent of N. That is, the high-frequency limit is reached.

Recently experimental verification of the predictions from these microwave calculations has been achieved for low field powers at Sandia National Laboratories (Reference 3). The experiment measures the nonexponential region of the current growth after application of a fast rising microwave field, and the neutral pressures in the experiment are low enough (.1 to 1 Torr) that the region of nonexponential electron density growth is measureable. Figure 26 is a preliminary comparison of the calculations and the experiment for an E/N of 800 Td and a field frequency of about 3 GHz. The good comparison of the calculations with the experiment is as much a test of the input cross section data as it is a test of the model used to calculate the ionization rates. It is gratifying in any case to see such good comparisons.
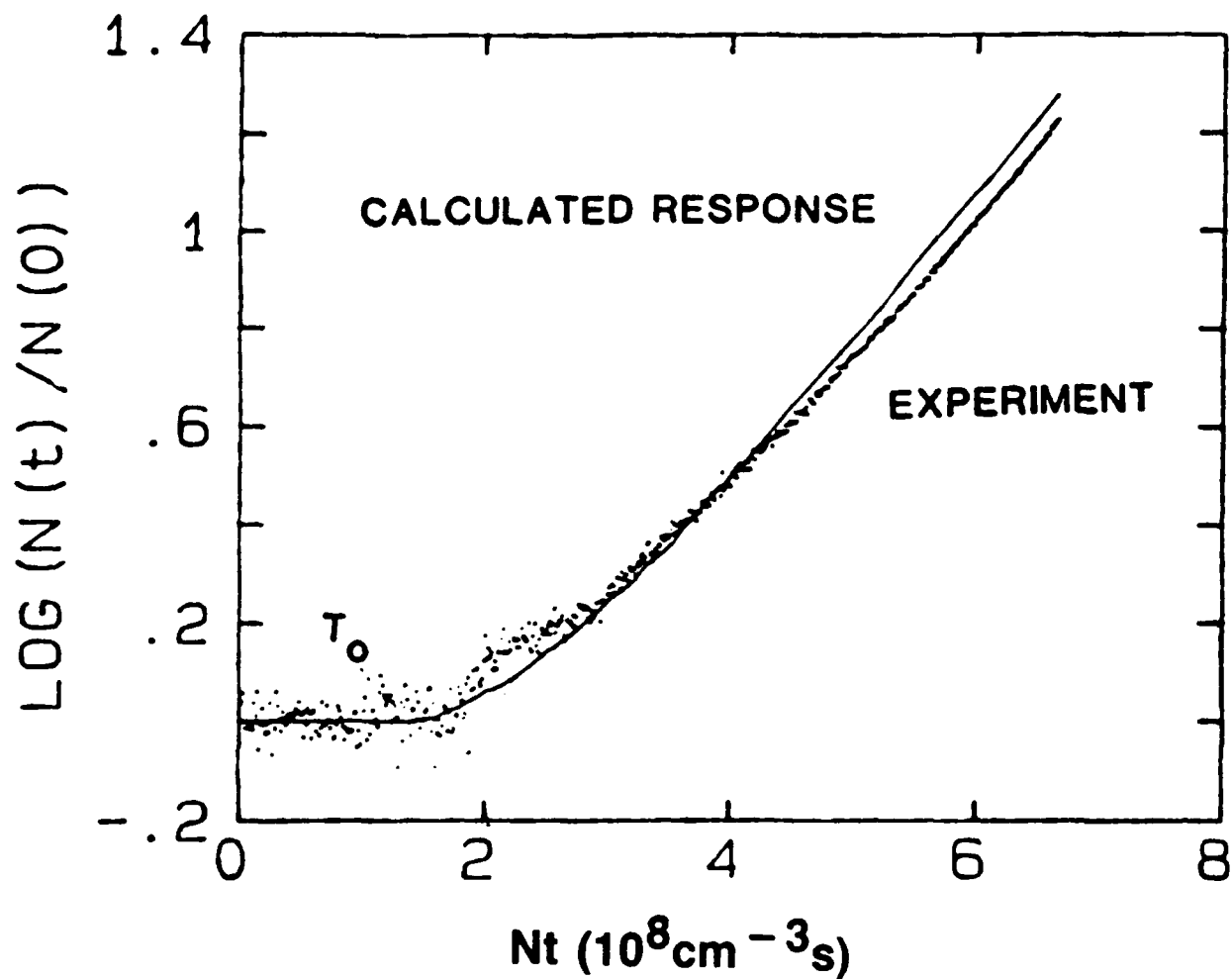
Figure 26. Comparision of calculated and experimental growth of current for the Sandia experiment at 800 Td, 3 GHz and .1 Torr.

V. Hydrodynamic-like Models

In this section we discuss the several attempts made to parameterize the time-dependence of the transport and rate coefficients appearing in the electron continuity eq.(4) in such a way that the results from one calculation or measurement can be scaled to another. Lacking such a scaling or parameterization, we are forced to perform the calculations or the measurements for each specific time-dependent field.

It is useful to distinguish two types of time-dependent phenomena ; the relaxation of the EEDF near a boundary or source of electrons and electron transport in a time-dependent field. When sources are present, the EEDF will depend on those sources and a general parameterization for arbitrary sources seems unlikely to be found. However, in the absence of sources or boundaries, but when the field is time-dependent, some parameterization may be possible.

The validity of the local field approximation has been questioned by many previous workers and several attempts have been made to find a way to "fix" the local field approximation. However, most of these efforts have been in the context of both the cathode boundary and the spatially varying field in the cathode fall of a steady-state discharge. Several years ago Chen and Phelps (Reference 39) took into account the low ionization coefficient near the cathode by including a finite turn-on or relaxation distance for the ionization rate after which the ionization rate was assumed to follow the local field. Addressing a similar problem, Marode and his colleagues (Reference 32) parameterized the ionization rate by the average electron energy which was allowed to increase in a prescribed way in the cathode fall region. This parameterization assumes that all EEDF moments follow the spatial variation of the average electron energy. Later, an English and French group (Reference 40) proposed a "memory-modified" field parameterization of the non-local ionization rate due to both field gradients in the cathode fall and the cathode boundary. Ingold has developed ways to approximate the collision terms in the space and time dependent moment equations which, in principle, yield the de-

sired results (Reference 31). All of these approaches are somewhat empirical but they do address the problem of a non-local dependence on the field and provide models in a limited parameter range of the non-uniform field electron transport.

Models to include time-dependence in the macroscopic parameters of a hydrodynamic-like model have also been attempted. To include the effects of a time-dependent field on the ionization rate coefficient, Longmire assumed that the collision terms in the first three moment equations are well-approximated by the constant collision frequency model (Reference 33). He then allowed the three time constants appearing in the three moment equations to be functions of the (time-dependent) average electron energy. Thus, the average electron energy replaces E/N as the parameter in this model. It was seen earlier that at late times in the relaxation and for a constant collision frequency model, this is a valid parameterization, but its validity is restricted to those conditions. This model is identical in principle to the moment methods of Ingold and Marode but differs in which parameters are assumed known and which are calculated. Aleksandrov, et al (Reference 41) present an interesting approach discussed in detail below which is identical in form to the result of Thornber (Reference 42) for the same problem in electron transport in semiconductors.

The works of Thornber and Aleksandrov give a form for each of the time-dependent transport coefficients that looks like a Taylor series in the powers of the time-derivative of the field. The coefficients of the time-derivatives are functions of the local field, E(Nt)/N. Although the motivation for the parameterization by Aleksandrov and Thornber differ from each other and from the motivation suggested here, the results are equivalent. The parameterization of Aleksandrov and Thornber is at first sight very appealing because the definition of a transport coefficient is through the relation (Reference 43),

$$Flux = Transport\ Coefficient \times Gradient$$

Thus, any gradient in the system will produce a flux in an attempt to smooth the gradient. If the time derivative of the field is considered as a gradient, there should be nonclassical fluxes in response to that gradient. Following this idea, the flux in the electron continuity equation is the sum of a flux due to the gradient in the electron density, the standard electron transport mechanism, and a flux due to the time-dependent field. Such a model is very attractive; it provides a computational scheme for the new transport coefficients and it provides a way to generalize experimental or computational results. In addition, this parameterization preserves the scaling with $E(Nt)/N$. The proposed form of the continuity equation is,

$$
\frac{\partial n_e}{\partial Nt} = \left(\frac{\nu_i}{N} \left(\frac{E(Nt)}{N} \right) + \gamma_0 \left(\frac{E(Nt)}{N} \right) \frac{\partial (E(Nt)/N)}{\partial Nt} \right) n_e
$$

$$
+ \left(\nu_d \left(\frac{E(Nt)}{N} \right) + \gamma_1 \left(\frac{E(Nt)}{N} \right) \frac{\partial (E(Nt)/N)}{\partial Nt} \right) \frac{\partial n_e}{\partial Nz}
$$

$$
+ \left(D_L N \left(\frac{E(Nt)}{N} \right) + \gamma_2 \left(\frac{E(Nt)}{N} \right) \frac{\partial (E(Nt)/N)}{\partial Nt} \right) \frac{\partial^2 n_e}{\partial (Nz)^2} \tag{28}
$$

where the γ's are the new transport coefficients and all transport coefficients depend only on the local field. To be useful, this model must provide us with a scheme for calculating the γ's. The hydrodynamic-like version of eq.(6) includes the additional gradient,

$$
f(\vec{r}, \vec{v}, t) = \sum_{\substack{i=0,1 \\ j}} f^{(i,j)}(\vec{v}) \left(\frac{\partial (E(Nt)/N)^i}{\partial (Nt)^i} \right) \otimes (-\nabla)^j n_e(\vec{r}, t) \tag{29}
$$

Equations for the evolution of the $f^{(i,j)}$'s can be found by combining eqs. (29) and (7),

$$
[a \cdot \nabla_v - C] f^{(0,0)}(\vec{v}) = 0
$$

$$
[a \cdot \nabla_v - C] f^{(1,0)}(\vec{v}) = \frac{\partial f^{(0,0)}(\vec{v})}{\partial (E/N)} \tag{30}
$$

The γ_i coefficients can be found,

$$\gamma_0 = \int C \, [f^{(1,0)}(\vec{v})] \, dv \qquad (31a)$$

$$\gamma_1 = \int v_z \, f^{(1,0)}(\vec{v}) \, dv \qquad (31b)$$

The form of the equations for (30) and (31) are similar to the equations for the $f^{(i)}$'s in the hydrodynamic formalism. We solved for the γ coefficients using a hydrodynamic code.

These results for the γ's can be compared with the "measured" values from the full time-dependent Boltzmann calculations. The difference between the full Boltzmann results and the local field values for the drift velocity are shown in Fig. 27 for a constant cross section model with elastic scattering only and a mass ratio of .1. The time dependence of the field was,

$$\frac{E(Nt)}{N} = \frac{E(Nt=0)}{N} \, (1 - \exp(-\beta Nt))$$

and the initial EEDF was the steady-state EEDF at .5 Td. This choice of the initial EEDF eliminates consideration of boundaries or sources and the departures from the local field values are due only to the time-dependent field.

From these calculations we can "measure" γ_1,

$$\gamma_1 = [v_d(t) - v_d(E(Nt)/N)] \, / \, \frac{\partial E(Nt)/N}{\partial Nt} \qquad (32)$$
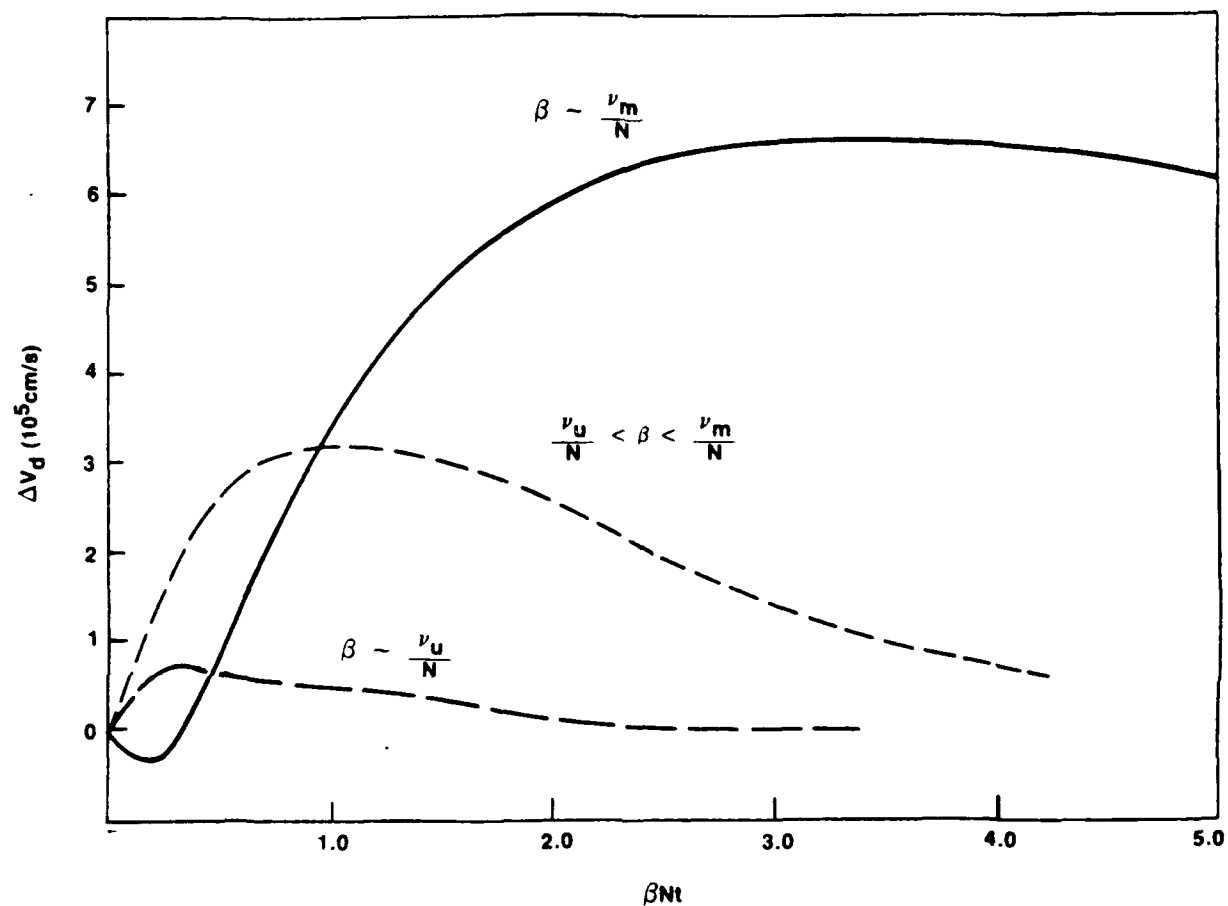
67

Figure 27. Difference between the drift velocity from the Boltzmann calculation and the local field value for three different time-dependent fields as a function of the dimensionless time βNt.

The "measured" values of γ_1 are compared in Fig. 28 with the calculated value from eq.(32). The measurements show that the γ_1's are not independent of $d(E(t)/N)/d(Nt)$ as required by the first order theory presented above to be valid. A second order theory fits the data better but not over the entire parameter range. We were not encouraged from these results to proceed to any higher orders even though the calculated value of γ_1 from eq.(31b) are close to the measured value as is seen in the figure.

Aleksandrov and Thornber give numerical values of the γ coefficients for certain cases but make no comparison with any "measured" values. They have also extended these ideas to the case of spatial gradients, and it is possible that the theory is more appropriate for the spatially varying field than for the time-dependent field.
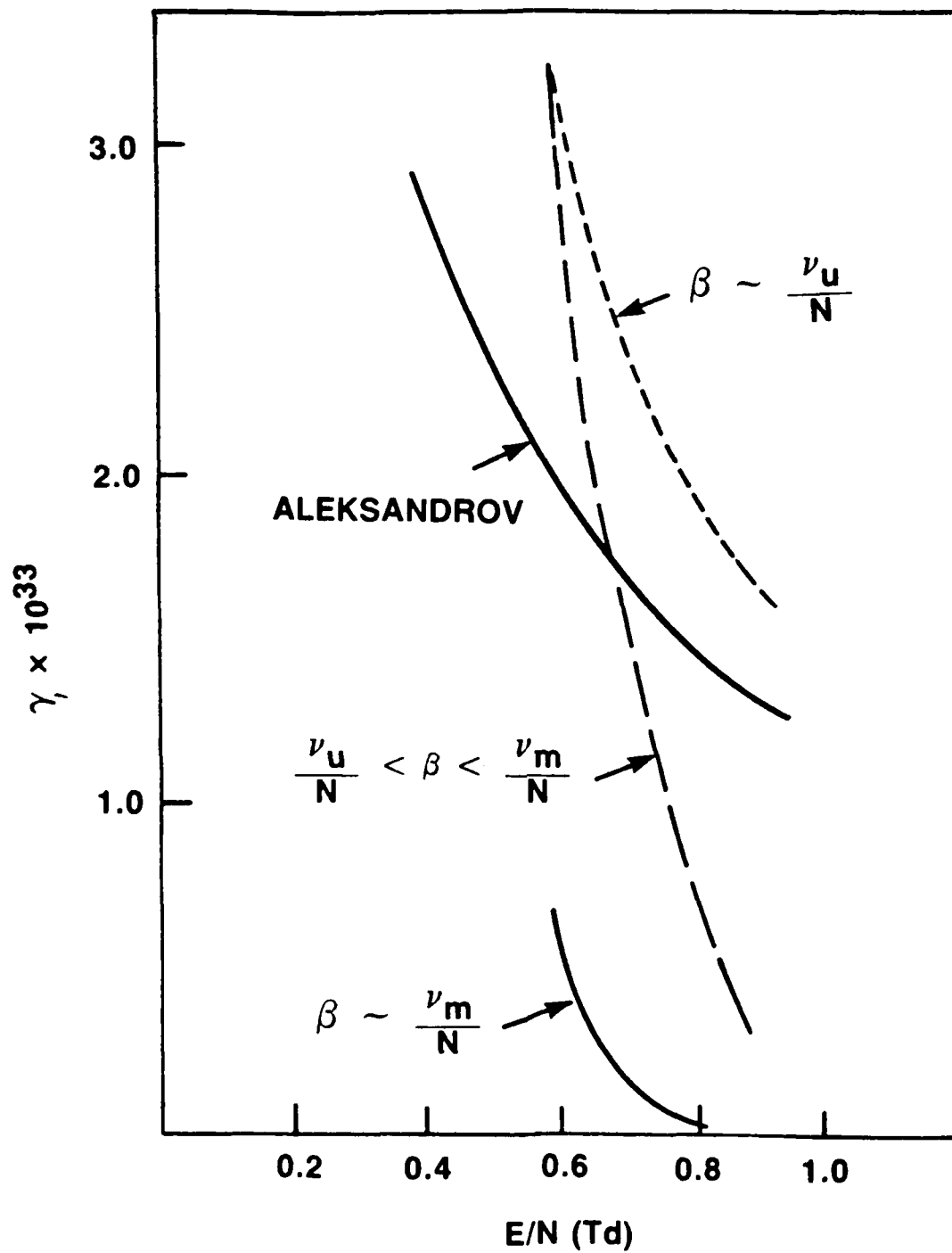
Figure 28. Comparison of calculated and "measured" value of γ_1 from eq.(32) and Fig. 27.

VI.   Summary and Conclusions

We have presented a numerical solution of the time-dependent Boltzmann equation and have illustrated its use with model calculations. These model calculations are relatively fast computationally and much easier to consider for analysis than the more realistic cross section models. A summary of the results of the calculations in nitrogen is presented, but the results differ only in detail from the model calculations. The model calculations serve to illustrate all the transient phenomena seen in tne more detailed calculations.

Based on the previously published results and those presented here, sources can be neglected for $Nt > (\nu_u/N)^{-1}$. The electrons lose memory of their initial conditions for times greater than the energy exchange time. Previous calculations and those presented here show that this relaxation time can vary orders of magnitude depending on the gas composition and E/N. Limits on the applicability of the local field approximation have been explored. Except for $E(Nt)/N$'s which vary rapidly on the scale of several times the energy exchange frequency, the local field is a valid parameter for the coefficients in the electron continuity equation.

Several attempts have been made to find a parameterization of the time-dependent transport and rate coefficients, or to formulate a hydrodynamic-like model for time-dependent fields. Previous efforts, to describe, for example, the ionization rate in the nonuniform field region of a discharge, have been examined for application in the time-dependent problem. We have not succeeded in finding such a macroscopic description for the time-dependent cases.

The electron continuity equation, only requires information on the electron density growth (or decay) constants and the electron flux. By restricting the information sought in the EEDF to the growth constants and the flux, phenomena which may be important in some applications are not observed. For example, while the net electron current is sensibly directed toward the anode throughout the relaxation of the EEDF, there is a component of the current

71

which flows to the catnode and which consists of the low velocity electrons. The moments which are most sensitive to this component are not usually included in models of gas discharges. This problem is similar to that expected in electron runaway. If the bulk distribution dominates the runaway component at all times due to ionization, the moments and information required in the continuity equation are independent of the runaway flux. This arguement suggests that in certain applications, a description based solely on the continuity equation is of limited utility. This problem has been recognized before, but a systematic attempt to resolve it has not been made.

Many previous Boltzmann calculations of the time-dependence of the EEDF's have been published. A good review is given in Wilhelm and Winkler (Reference 7). As was mentioned in the introduction, the previous time-dependent Boltzmann calculations have assumed a two-term approximation and that the anisotropic component of the distribution is in equilibrium with the isotropic part; i.e., $\partial f_1/\partial t = 0$. Although the calculations discussed above are all two-term results, we have performed multi-term calculations as spot checks along the way to verify that the error introduced by the two-term approximation is no more severe in the transient regime than it is in the steady-state regime. This has been verified in all the model cases and in nitrogen. The neglect of the time derivative of f_1 is a good approximation for the most part. However, if the detailed response of an electron swarm to an rf field is desired, the neglect of the time derivative is no longer justified. For example, there is no phase shift between the applied voltage and the current if $\partial f_1/\partial t = 0$.

Again, due to the particular form of the Boltzmann equation commonly used with the two-term approximation, a single second order differential equation for f_0 in the place of two coupled first order differential equations for f_0 and f_1, the drift velocity overshoots and undershoots and the cathode-directed component of the current have not been previously reported in the gas discharge literature.

72

Electron transport in semiconductors is described by a model which is formally equivalent to that used here (Reference 1). There the phenomena of drift velocity overshoot and undershoots have been inferred from measurements of the frequency dependence of the conductivity in semiconductors. Considerable theoretical effort has been devoted to the explanation, and the phenomena we see here are consistent with the explanations given in that literature. We anticipate that there should also be a cathode-directed component of the current associated with the transient electron transport in semiconductors. It is interesting to speculate as to the effect of this current component in fast switching in semiconductors.

In a separate effort but related to this work we have begun Monte Carlo calculations of electron transport in nonuniform fields in space (Reference 6). All the phenomena seen in the transient regime are also seen in the nonuniform field regions. The explanations for the effects are directly analagous to the explanations in spatially varying fields are directly analagous to the explanations given here for the time-dependent fields. It is tempting to speculate that through the judicious tailoring of the field distributions in space or the time-dependence of the applied voltage that we can tailor a electron energy distribution function to fill specific requirements for specific applications.

References

1. Carlo Jacoboni and Lino Reggiani, Rev. Mod. Phys., 55, 725 (1983).

2. A.D. MacDonald, Microwave Breakdown in Gases, (John Wiley and Sons, New York, 1966).

3. G.N. Hays, J.B. Gerardo, L.C. Pitchford and J.T. Verdeyen, 37th Gaseous Electronics Conference, GE-1, 1984.

4. J. Dutton, J. Phys. Chem. Ref. Data, 4, 577 (1975).

5. J.W. Gallagher, E.C. Beaty, J. Dutton and L.C. Pitchford, J. Phys. Chem. Ref. Data, 12, 109 (1983).

6. T.J. Moratz and L.C. Pitchford, 37th Gaseous Electronics Conference, JA-3, 1984.

7. J. Wilhelm and R. Winkler, J. de Phys. C7, supp. 7, C7-251 (1979).

8. A. Mozumber, J. Chem. Phys., 72, 1657 (1980).

9. J.-S. Chang, R.M. Hobson, J.G. Laframboise and G.L. Ogram, J. Phys. B. 11, 1675 (1978).

10. C.F. Eaton and L.H. Holway, Phys. Rev., 143, 48 (1965).

11. G.L. Braglia, Il Nuovo Cim. 25B, 479 (1975).

12. L.H. Holway, Jr., Phys. Fluids 16, 35 (1967).

13. K.Anderson and K.E. Shuler, J.Chem. Phys., 40, 633 (1964).

14. J. Wilhelm and R. Winkler, Beit. Plasmaphys., 16, 287 (1976); Ann. Phys., 34, 119, (1977); Beit. Plasmaphys., 17, 369 (1977); Beit. Plasmaphys., 20, 225 (1980).

15. G.L. Braglia, Il Nuovo Cim., 58, 352 (1968); G.L. Braglia and L. Ferrari, Il Nuovo Cim., 67, 167 (1970); G.L. Braglia and L. Ferrari, Il Nuovo Cim., 4B, 262 (1971); G.L. Braglia, G.L. Caraffin, and M. Diligenti, Il Nuovo Cim., 62B, 139 (1981).

16. Y. Sakai, H. Tagashira and S. Sakamoto, J. Phys. D, 10, 1035 (1977); K. Kitamori, H. Tagashira and Y. Sakai, J. Phys. D, 11, 283 (1978).

17. H. Tagashira, Y. Sakai and S. Sakamoto, J. Phys. D, 10, 1051 (1977).

18. J. Wilhelm and R. Winkler, Ann. Phys., 36, 103 (1979); Beit. Plasmaphys., 18, 317 (1978).

19. W.L. Morgan, 1979, JILA Information Center Report No. 19, Boulder, Co.; S.D. Rockwood and A.E. Greene, Comp. Phys. Comm., 19, 377 (1980).

20. W.P. Allis, in Handbuch der Physik, ed. S. Flugge (Springer, Berlin, 1956), Vol. 21, p 383.

21. Kailash Kumar, H.R. Skullerud and R.E. Robson, Aust. J. Phys. 33, 343 (1980).

22. A.V. Phelps and L.C. Pitchford, "Anisotropic scattering of electrons by N2 and its effect on electron transport", submitted to Phys. Rev. A, (1984).

23 Kailash Kumar, J. Phys. D., 14, 2199 (1981).

24. L.C. Pitchford, S.V. ONeil and J.R. Rumble, Jr., Phys. Rev. A 23, 294 (1981); L.C. Pitchford and A.V. Phelps, Phys. Rev. A, 25, 540 (1982).

25. T. Holstein, Phys. Rev. 70, 367 (1946).

26. S. Yoshida, A.V. Phelps and L.C. Pitchford, Phys. Rev. A 27, 2858 (1983).

27. L.F. Shampine and H.A. Watts, "DEPAC - Design of a User Oriented Package of ODE Solvers", Sandia National Laboratories Report SAND79-2374 (September 1980).

28. J. Wilhelm and R. Winkler, Beit. Plasmaphys., 23, 483 (1983).

29. L.C. Pitchford and T.A. Green, 36th Gaseous Electronics Conference, C-6,1983.

30. I.P. Shkarofsky, T.W. Johnston, and M.P. Bachynski, The Particle Kinetics of Plasmas (Addison-Wesley, Reading, 1966).

31. L.C. Pitchford and J. Ingold, 37th Gaseous Electronics Conference, JA-4, 1984; J.H. Ingold, J. Appl. Phys., 40, 55 (1969).

32. Tran Ngoc An, E. Marode and P.C. Johnson, J. Phys. D., 10, 2317 (1977).

33. C. Longmire, Reported by R.S. Cabayan, May 1983 memorandum "Summary of Discussions During High-Power Microwave Air Breakdown Workshop at Lawrence Livermore National Laboratories, February 18, 1983".

34. I.D. Reid, Aust. J. Phys., 32, 231 (1979).

35. A.V. Phelps and L.C. Pitchford, JILA Information Center Report No. 26 (1984), unpublished.

36. D. Rapp and P. Englander-Golden, J.Chem. Phys., 43, 1464 (1965).

37. A.V. Phelps, "Theory of Growth of Ionization During Laser Breakdown", in Physics of Quantum Electronics, eds. Kelley, Lax and Tannenwald, McGraw Hill, 1966, p.538.

38. L.C. Pitchford, "Gas Breakdown in High-Power, Fast-Rising Microwave Fields", Sandia National Laboratories Internal Memorandum, July 1984.

39. A.V. Phelps, private communication.

40. J.P. Boeuf, A.J. Davies, J.G. Evans, E. Marode and P. Segur, Seventh International Conference on Gas Discharges and their Applications, London, 1982.

41. N.L. Aleksandrov, A.P. Napartovich and A.N. Starostin, Sov. J. Plasma Phys. 6, 618 (1980).

42. K.K. Thornber, IEEE Elec. Dev. Lett., EDL-3, 69 (1982); J. Appl. Phys., 51, 2127 (1980); J. Appl. Phys., 52, 279 (1981).

43. H.J.M. Hanley, Transport Phenomena in Fluids, (Marcel Dekker, Inc., New York, 1969).

77

END

FILMED

8-85

DTIC